Mathematical Optimisation of the Suspension System of an Off-Road Vehicle for Ride Comfort and Handling

by

Michael John Thoresson

Submitted in partial fulfilment of the requirements for the degree

Master of Engineering

in the Faculty of

Engineering, Built Environment and Information Technology

University of Pretoria, Pretoria

November 2003

Mathematical Optimisation of the Suspension System of an Off-Road Vehicle for Ride Comfort and Handling

Michael John Thoresson

Supervisor:	Mr. P.S. Els
Co-Supervisors:	Prof. J.A. Snyman and Dr. P.E. Uys
Department:	Mechanical and Aeronautical Engineering
Degree:	Master of Engineering

Abstract

This study aims to evaluate the use of mathematical optimisation algorithms for the optimisation of a vehicle's spring and damper characteristics, with respect to ride comfort and handling.

Traditionally the design of a vehicle's suspension spring and damper characteristics are determined by a few simple planar model calculations, followed by extensive trial-and-error simulation or track testing. With the current advanced multi-body dynamics computer software packages available to the design engineer, the integration of traditional mathematical optimisation techniques with these packages, can lead to much faster product development. This, in turn results in a reduction of development costs.

A sports utility vehicle is modelled by means of a general-purpose computer programme for the dynamic analysis of a multi-body mechanical system. This model is validated against measurements from road tests. The mathematical model is coupled to two gradient-based mathematical optimisation algorithms. The performance of the recently proposed Dynamic-Q optimisation algorithm, is compared with that of the industry-standard gradient based Sequential Quadratic Programming method. The use of different

finite difference approximations for the gradient vector evaluation is also investigated.

The results of this study indicate that gradient-based mathematical optimisation methods may indeed be successfully integrated with a multi-body dynamics analysis computer program for the optimisation of a vehicle's suspension system. The results in a significant improvement in the ride comfort as well as handling of the vehicle.

Keywords : mathematical optimisation, vehicle suspension, spring and damper characteristics, SQP, Dynamic-Q, ride comfort, handling.

Wiskundige Optimering van die Suspensiestelsel van 'n Veldvoertuig vir Ritgemak en Hantering

Michael John Thoresson

Studieleier:	Mnr. P.S. Els
Mede-leiers:	Prof. J.A. Snyman en Dr. P.E. Uys
Departement:	Meganiese en Lugvaartkundige Ingenieurswese
Graad:	Magister in Ingenieurswese

Opsomming

Die doel van hierdie studie is om wiskundige optimeringsalgoritmes te evalueer met die oog op die optimering van 'n voertuigsuspensiestelsel se veer- en demperkarakteristieke vir beide ritgemak en hantering.

Die praktyk by ontwerp van voertuigsuspensies, is om veer- en demperkarakteristieke te bepaal aan die hand van vereenvoudigde twee-dimensionele modelberekenings gevolg deur intensiewe probeer-en-tref simulasies en/of padtoetse. Integrasie van bestaande gevorderde multi-liggaam dimanika rekenaar pakette met beskikbare wiskundige optimeringstegnieke, kan produkontwikkeling versnel en baie koste bespaar.

Vir die doeleindes van hierdie ondersoek word 'n ontspanningsvoertuig gemodelleer met behulp van 'n veeldoelige rekenaarprogram vir die dinamiese analise van meganiese stelsels. Die simulasieresultate van die model word gevalideer aan die hand van padtoetse. Die rekenaarmodel word daarna gekoppel aan gradiënt -gebaseerde wiskundige optimeringsalgoritmes.

Om die effektiwiteit van optimeringsalgoritmes vir die optimering van suspensiekarakteristieke te evalueer, word die voorgestelde Dynamic-Q algoritme vergelyk met die standaard Opeenvolgende Kwadratiese Programmering (SQP)- metode. Die gebruik van verskillende benaderings vir die berekening van die gradiëntvektor in Dynamic-Q word ook ondersoek.

Uit die ondersoek blyk dat gradiëntgebaseerde wiskundige optimeringsmetodes suksesvol met multi-liggaam dinamika pakette geïntegreer kan word vir

die optimering van 'n voertuig se suspensiestelsel. Dit het 'n aansienlike verbetering in ritgemak en hantering van die voertuig tot gevolg.

Sleutelwoorde : wiskundige optimering, voertuigsuspensie, veer- en demperkarakteristieke, SQP, Dynamic-Q, ritgemak, hantering.

Acknowledgments

- Optimisation related investigations were performed under the auspices of the Multi-disciplinary Optimisation Group (MDOG) of the Department of Mechanical and Aeronautical Engineering of the University of Pretoria.
- The vehicle dynamics simulation for the design of the controllable suspension system is based upon work supported by the European Research Office of the US Army under Contract No. N68171-01-M-5852.
- National Research Foundation (NRF) grant for funding of the optimisation related investigations.
- Land Mobility Technologies (LMT) for vehicle testing assistance and supplying tyre data.
- Land Rover South Africa for supplying test vehicles.
- My study leaders Prof Snyman, Dr Uys, and Mr Els for their continual support and enthusiasm throughout this research.
- My parents for their continual support and encouragement throughout my studies.

CONTENTS

LIST OF TABLES

LIST OF FIGURES

LIST OF ABBREVIATIONS

AAP	Average Absorbed Power
ANN	Artificial Neural Network
apg	Abberdene Proving Ground
BFGS	Broyden-Fletcher-Goldfarb-Shanno
BS	British Standard
cfd	Central Finite Difference
CFD	Computational Fluid Dynamics
cg	Center of Gravity
DFP	Davidon-Fletcher-Powell
FEM	Finite Element Method
ffd	Forward Finite Difference
GA's	Genetic Algorithms
inf	Infeasible Starting Point
ISO	The International Organisation for Standardisation
LFOP	Leap-Frog Optimiser
LFOPC	Leap-Frog Optimiser for Constrained Problems
LMT	Land Mobility Technologies
MDOG	Multi-disciplinary Optimisation Group
NRF	National Research Foundation
PSD	Power Spectral Density
RMS	Root Mean Square
SLP	Sequential Linear Programming
SQP	Sequential Quadratic Programming
SUV	Sports Utility Vehicle
VDV	Vibration Dose Value

LIST OF SYMBOLS

A	Piston Area
$\mathbf{A}$	Dynamic-Q Hessian Matrix
a	Curvature
a_{RMS}	Root Mean Square Acceleration
a_w	Weighted Acceleration
a_y	Lateral Acceleration
d	Displacement Error
$dpsf$	Damper Scale Factor
$dpsff$	Damper Scale Factor Front
$dpsfr$	Damper Scale Factor Rear
dx_k	Perturbation in Design Variable k
$f(\mathbf{x})$	Objective Function
$f(\mathbf{x}^*)$	Optimum Objective Function Value
F	Force
$F(v)$	Damper Force
$F(\mathbf{x})$	Multi-Variable Function
F_c	Current Force
F_s	Static Force
G_{a_y}	Lateral Acceleration Gain
G_{do}	Road Roughness Coefficient
G_{dr}	Road Displacement Power Spectral Density
$g_j(\mathbf{x})$	Inequality Constraint Functions
G_{Y_w}	Yaw Velocity Gain
$gvol$	Static Gas Volume
$gvolf$	Static Gas Volume Front
$gvolr$	Static Gas Volume Rear

$h_j(\mathbf{x})$	Equality Constraint Functions
H_k	Hessian Matrix at Iteration k
$\mathbf{I}$	Identity Matrix
k	Constant
K	Steering Angle Gain
l	Driver Preview Distance
m	Number of Inequality Constraints
n	Number of Design Variables
N	Population Size for Genetic Algorithms
n	Spatial Frequency
P	Current Pressure
P_o	Static Gas Pressure
r	Number of Equality Constraints
R	Piston Radius
S	Total Strut Stroke
s	Vehicle Speed
t	Time
T	Total Sample Time
V	Current Volume
v	Velocity
V_{1-8}	Damper Definition Variables
V_o	Static Gas Volume
VDV	Vibration Dose Value
x	Relative Displacement
x_k	Design Variable k
x_o	Initial Piston Height
x_s	Static Spring Displacement
$\mathbf{x}$	Design Variables Vector

$\mathbf{x}^*$	Optimum Design Variables Vector
Y_w	Yaw Velocity
β_{0-3}	Characteristic Damper Coefficients
δ	Steering Angle
γ	Gas Constant
ω	Terrain Index
τ	Driver Preview Time

1. INTRODUCTION

One of the fastest growing sectors in the vehicle market is currently the Sports Utility Vehicle (SUV) sector. This sector includes vehicles ranging from baseline to luxury units, with manufacturers such as Toyota, Mercedes-Benz and Porsche offering SUV's. The biggest problem with these vehicles is that the owners expect the luxury and comfort associated with a large luxury vehicle, while still demanding good off-road tractability and sports car on-road handling performance.

Since the invention of the motor vehicle, the suspensions used have always represented a compromise between ride comfort and handling. Good ride comfort requires a supple (soft) suspension, whilst good handling requires a stiff (hard) suspension. This compromise has been reduced in newer passenger vehicles by the addition of anti-roll bars, to stiffen the suspension for handling manœuvres, while keeping a soft suspension for ride comfort. With the SUV's becoming luxury orientated, more emphasis is being placed on comfort, resulting in a vehicle that has good off-road tractability and good ride comfort, but poor on-road handling behaviour. With this configuration the driver and passengers can comfortably be transported at high speeds over poor road surfaces. An accident avoidance type manœuvre, can however not be performed safely, leading to vehicle roll-over in handling situations. The performance orientated SUV's have good ride comfort and reasonable on-road handling, but poor off-road capability. This thesis reports on the investigation of a novel suspension system, currently under development at the University of Pretoria, which aims to avoid these traditional compromises in the design of suspension systems.

Traditionally suspension spring and damper characteristics are determined by a few simple planar model calculations and many trial-and-error

simulations or road tests of a prototype vehicle. The spring and damper characteristics undergo many changes before the final configuration is put into production. In today's competitive world, this type of time consuming design work is no longer acceptable, as it adds unnecessary development costs to the vehicle. Using modern advanced multi-body dynamics simulation software, designers have the ability to model the vehicle driving under almost all possible road conditions. The integration of an optimisation procedure with such simulation software, will enable the design engineer to determine the desired suspension damper and spring characteristics, with limited prototype testing.

A brief literature overview concerning vehicle dynamics, suspension optimisation and optimisation algorithms, is presented in Chapter 2. Chapter 3 deals with the optimisation problem at hand, with details of the mathematical model and its validation being given. In Chapter 4 the results are presented and discussed. Conclusions drawn from the study together with suggestions for future work to be performed are presented in the final two chapters. Appendix A provides a summary of an investigation into the handling objective function.

2. LITERATURE STUDY

2.1 Vehicle Dynamics

The vehicle under investigation is a very complex dynamical system, into which much thought must go, in order to develop a marketable and competitive vehicle. As illustrated in Figure 2.1 the response of the vehicle body depends on the vehicle's suspension response, and that in turn depends on the road input conditions. These road input conditions can be further complicated by the steering action of the driver.

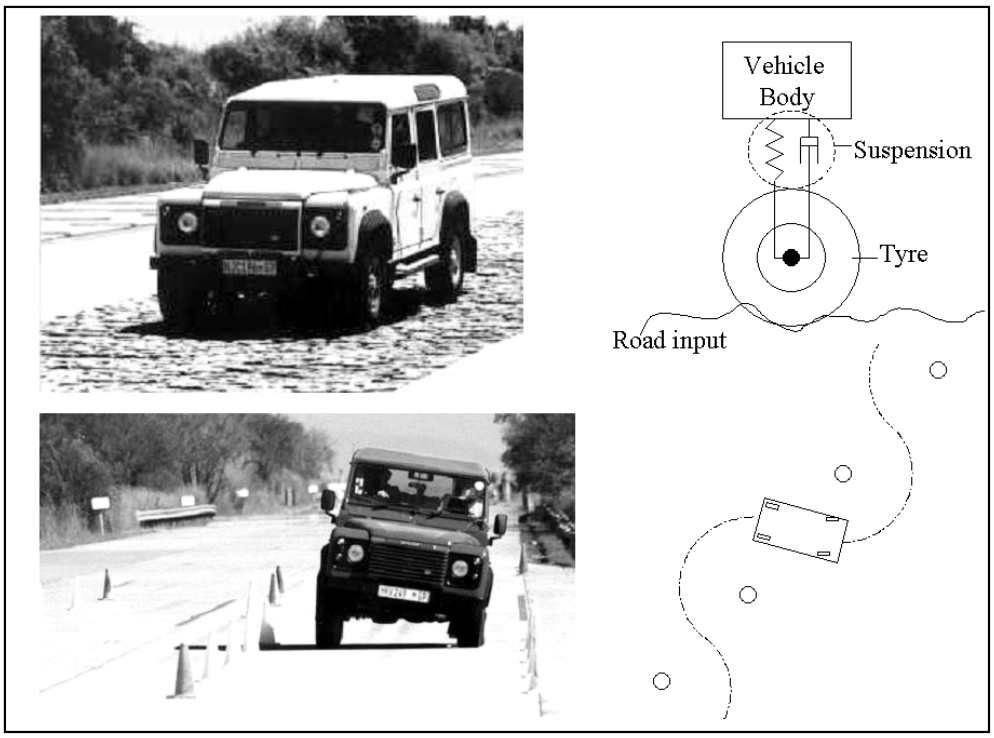

Figure 2.1: Vehicle response due to road and steering input

2.1.1 Road input

The road is the primary input to the vehicle system. Its condition affects the vehicle in a number of ways, ranging from ride comfort experienced by the vehicle passengers and driver, to roll-over, trip-up, and road banking affecting the vehicle's cornering performance. It is therefore important to take cognizance that not all roads have smooth surfaces. Rather they are complex randomly irregular three dimensional profiles, that may exhibit a certain degree of harmonic profiles, like the sinusoidal corrugations commonly found on gravel roads or traffic speed bumps. In this study the road will be considered as a smooth plane for the handling requirements, and as a so-called Belgian paving for ride comfort requirements. The Belgian paving is a test track specially designed to excite all the vehicle's vibration modes for the purpose of ride comfort and endurance evaluations. The Belgian paving test track used is classified by using the ISO 8608 [1] standard. In terms of this standard it has a roughness coefficient G_{do} of 1e-4 $m^2/(cycles/m)$, and a terrain index ω of 4. These are obtained from the linear approximation that is applied to all road profiles where the power spectral density (PSD) function is defined as follows:

$$G_{dr} = G_{do} n^{-\omega} \tag{2.1}$$

where n is the spatial frequency. The power spectral density of the Belgian paving is included in Figure 2.2 with a photograph of the vehicle driving on the Belgian paving in Figure 2.1 top left corner.

2.1.2 Tyres

The tyre of a vehicle is one of the most important components of the vehicle model, as it serves as the interface between the vehicle and the road. Ideally it must maintain traction at all times, while absorbing most of the road irregularities. The tyre generates a lateral force which is necessary to keep the vehicle on track when travelling along a curve. It also generates longitudinal force which is the driving force that ensures that the vehicle can propel or brake when required. Self-aligning moments are also generated to ensure it

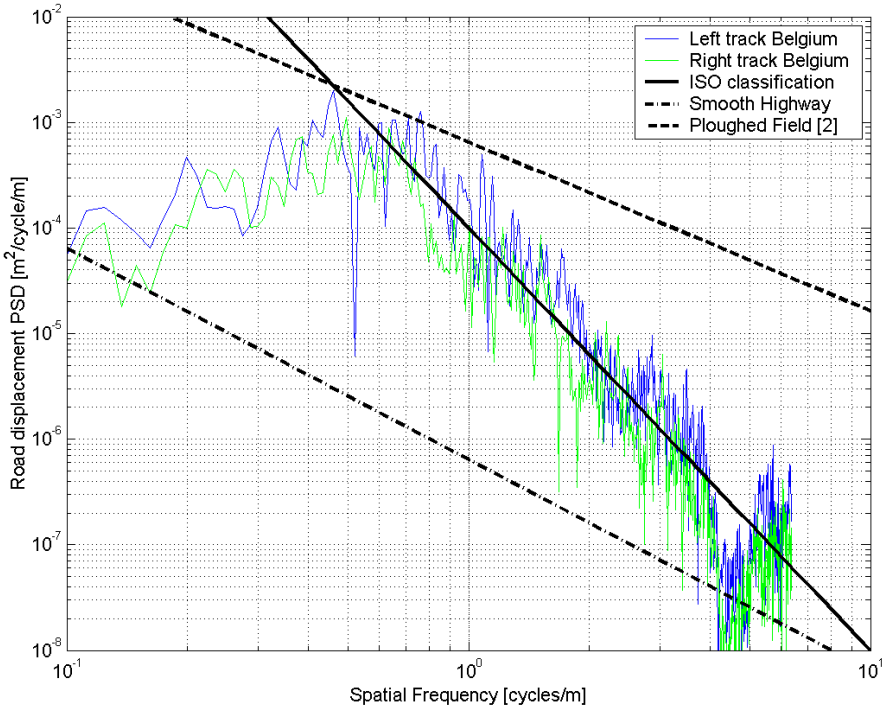

Figure 2.2: ISO 8608 classification PSD of Belgium paving test track

keeps following the desired path when road disturbances are encountered. Because of the wide range of functions the tyre must perform, it is equally difficult to model. In most vehicle dynamics simulations, the tyre model is the most limiting factor in achieving correlation with measured results. The tyre would filter out road irregularities shorter than the tyre contact patch, while the simple tyre models do not. The magic formula tyre model [3] is regarded as the industry standard for handling simulation, and in its latest form the swift tyre model [4, 5] is considered appropriate for rough road simulation. However, it has been difficult to obtain reliable coefficients, the determination of which require many tyre tests to be performed, to accurately model the real tyre [6]. The swift tyre makes use of the empirical magic formula model for handling, and a rigid ring model (Figure 2.3) for ride comfort. The recently proposed FTire [7] makes use of a flexible ring model, to more accurately describe the tyre road enveloping effects, for ride comfort. With computational time being more than 20 times real time, it becomes too expensive to use for optimisation. On the other hand, the Fiala tyre model

in ADAMS [4, 5] is a very simple model based on a linear approximation to the tyre data, but is normally not sufficiently accurate. It makes use of a sector type model. The middle of the way tyre model is the ADAMS 521 tyre, which makes use of lookup tables with the tyre characteristics, and has the option of a point follower tyre model (Figure 2.3) for ride comfort. This model is best for limited tyre test data, and does not require the fitting of complex coefficients.

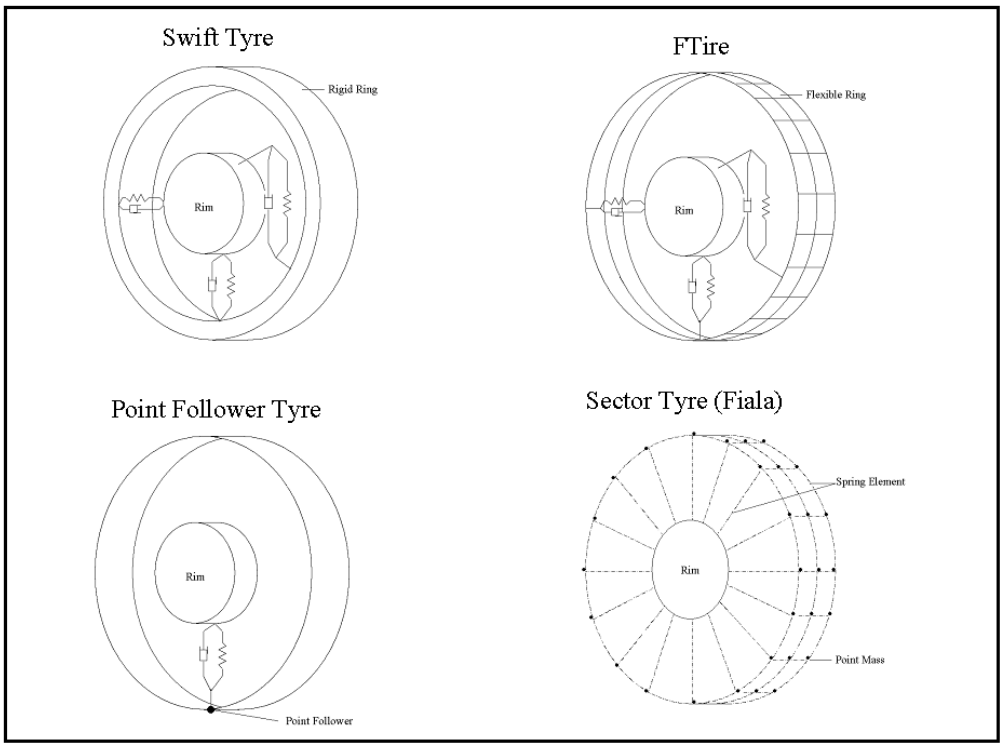

Figure 2.3: Tyre models

2.1.3 Suspension

Damper Characteristics

Although most textbook approaches to vehicle dynamics assume a linear relation between damper force and relative velocity, this is hardly the characteristic that a vehicle damper assumes. The vehicle damper is a very complicated non-linear element, thus being difficult to model mathematically. This can mainly be ascribed to the complex fluid dynamics occuring

inside the automotive damper. The characteristics of dampers are normally designed with switch over points, to try and minimize the traditional compromise between ride comfort and handling. The automotive damper is thus designed to have a high damping rate for low velocities associated with handling, and a low damping rate for higher velocities associated with vehicle ride comfort. A switch between these two settings is normally gradual in form. The fact that a damper effectively consists of various orifices, that restrict the flow of oil, and in doing so, generates a force, also needs to be considered. Oil flow through an orifice is normally described by a quadratic relationship. When optimising a vehicle required to perform various manœuvres, it becomes necessary to describe this non-linear damper behaviour in terms of a mathematical expression. It must also be kept in mind that the method used to evaluate the mathematical model, must be computationally inexpensive.

Complex Models:

There are many detailed damper models available that all aim to accurately describe the damper characteristics, but most of these models require data that are normally not available at the design stage, such as working oil temperature and pressure [8]. These models are normally time-consuming to fit to current damper data, and they will therefore not be further considered in this study.

Spline Approximation:

The Hermite spline has been used by Eberhard et al. [10] for the description of the damping characteristics of an automotive damper, in their optimisation process. They made use of five definition points and four gradient curves. A Hermite spline was then defined between two consecutive points, exhibiting the same gradient at these points. This was done for all the defined points of the damper characteristics as illustrated in Figure 2.4. Eberhard et al. [10], however, stated that:

> The constraints which have to be formulated to ensure physical feasibility are hard to handle and prevent complete automation of the approach.

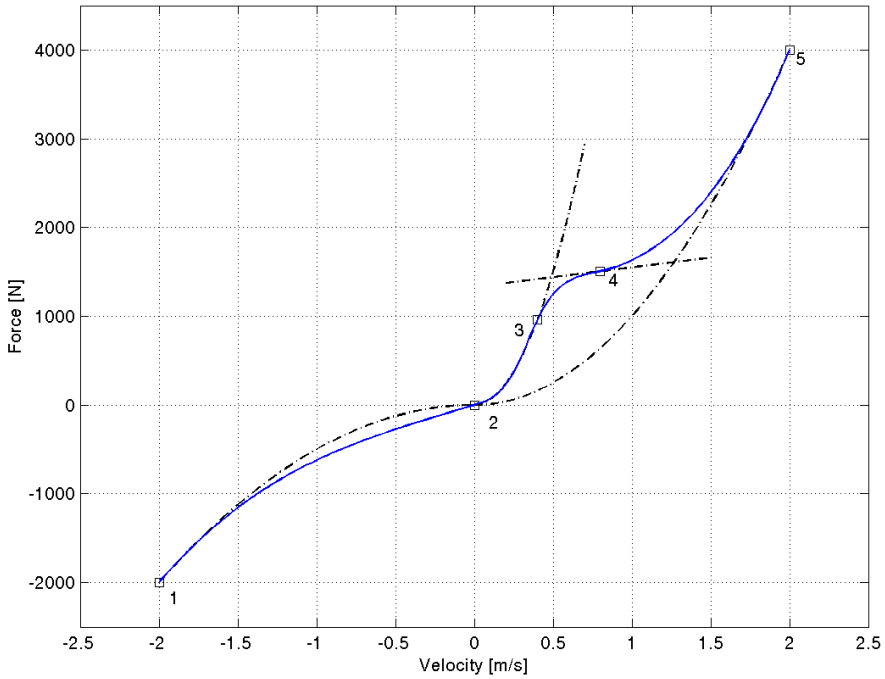

Figure 2.4: Hermite spline approximate damper characteristics [10]

Etman Damper Model:

Etman et al. [11] proposed an eight variable empirical curve fit method to specify the damper characteristics. This model consists of a function of four variables for compression, and four for rebound. The same function is used for both compression and rebound. The damper force is described as :

$$F(v) = \frac{\beta_0 v^2(\beta_1 - \beta_2 v)}{\beta_0 v^2 + \beta_1 - \beta_2 v} + \beta_3 v^2 \tag{2.2}$$

where F is the damper force, v the velocity and β_i, $i = 0, 1, 2, 3.$ are the characteristic coefficients. Etman et al. suggests the following ranges for the characteristic coefficients:

Variable	Compression	Rebound	Units
β_0	-22 - -0.3	0.3 - 22	$10^6 Ns^2m^{-2}$
β_1	-200 - -2	2 - 200	$10^3 N$
β_2	0.7 - 70	0.7 - 70	$10^3 Nsm^{-1}$

They found that β_3 has a limited contribution to the curve shapes, and thus kept it constant for optimisation. Attempts were made in this study to fit this model to the standard Land Rover damper characteristics. However, as this turned out to be troublesome, it was decided not to use this model for the optimisation process. The resulting characteristic for this model is illustrated in Figure 2.5.

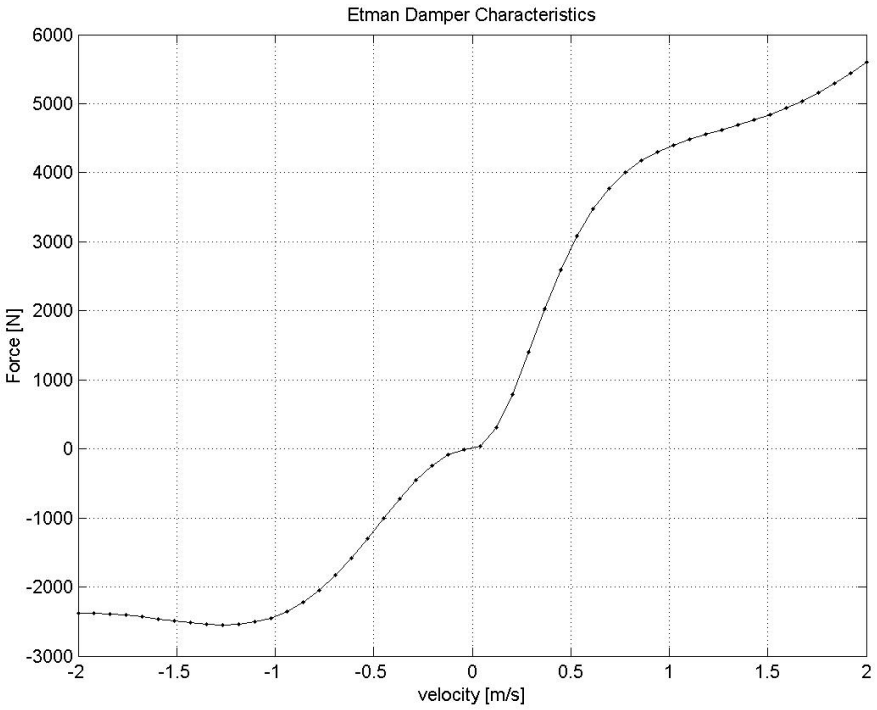

Figure 2.5: Etman damper model characteristics [11]

Piece-wise Linear Approximation:

Naude and Snyman [12, 13] and Naude [14] proposed a six piece-wise linear approximation (Figure 2.6) for the description of the damper characteristics for the optimisation of a pitch plane ride comfort vehicle model. Their study, however, indicates that a four piece-wise linear approximation may be sufficient. For this reason, the four piece-wise linear model is used in Section 3.6.3. where the optimisation of the hydro-pneumatic spring-damper is dicussed.

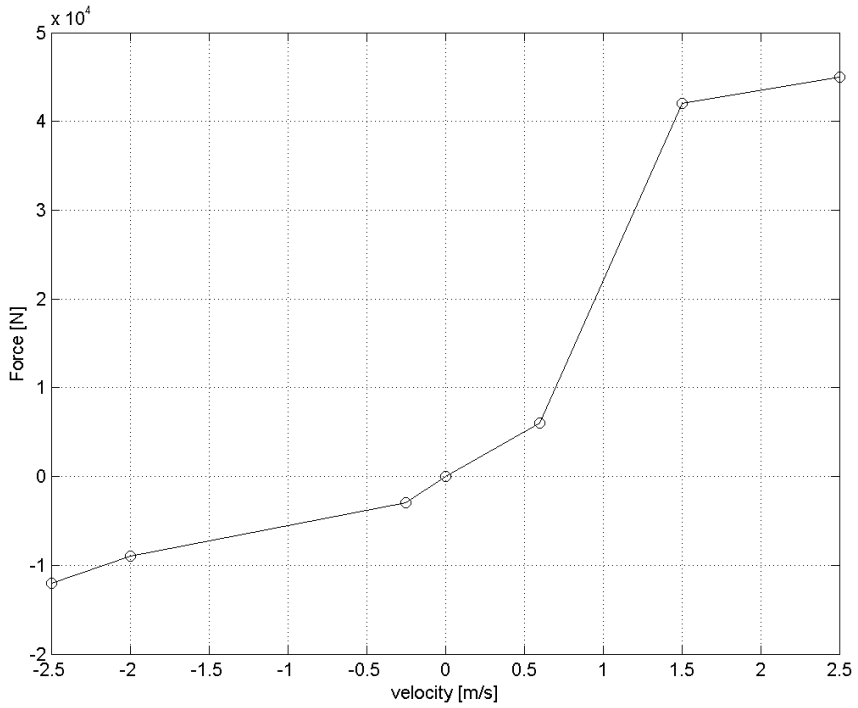

Figure 2.6: Six piece-wise linear damper model as used by Naude and Snyman [12]

Semi-active Hydro-pneumatic Suspension Unit

The design and implementation of a semi-active suspension system on a four wheel drive off-road leisure vehicle has been an ongoing research activity at the University of Pretoria. The suspension system consists of a two state semi-active damper and two state hydro-pneumatic spring.

Principle of Operation:

The semi-active spring-damper (shown schematically in Figure 2.7) incorporates two damper packs (fitted with bypass valves), and two gas accumulators, effectively giving two damper characteristics and two spring characteristics in a single suspension unit [15]. Switching between the two spring and damper characteristics is achieved by solenoid valves, as illustrated in Figure 2.7. Valve switching times vary between 50 and 100 milliseconds depending on system pressure. This means that spring and damper characteristics can be taken as design variables, to be optimised for both ride comfort

and handling respectively, by switching the suspension system to either the ride comfort or handling option, depending on the vehicle's operating conditions. Each operating setting is expected to have different optimum values for the spring and damper characteristics. This approach eliminates the traditional ride comfort versus handling compromise. With this capability the optimisation is done by treating the suspension unit as two passive systems. One for handling and one for ride comfort.

Refering to Figure 2.7 the handling condition of the suspension unit, is obtained when accumulator A and damper x are working, with all the solenoid valves (a, b and c) closed. If lower damping is required for the particular driving condition, solenoid valve a is opened resulting in a larger flow area in turn reducing the damper force. For the ride comfort setting, solenoid valves a and b would be closed and solenoid valve c would be open, thus creating a larger effective accumulator volume with both accumulator A and B working. This condition would result in a lower spring stiffness. Dampers x and y would be generating forces that can be lowered by opening solenoid valves a and b should the operating conditions require lower damping.

Spring Characteristics:

The spring force is generated by the compression and expansion of the nitrogen filled gas accumulator volume, resulting in very non-linear spring characteristics. The spring characteristics can be defined in terms of a simple relation between displacement and force, if the hysteresis effects are ignored. The system design variables are defined in Table 2.1. The piston area is defined as:

$$A = \pi R^2 \tag{2.3}$$

The static accumulator gas pressure is:

$$P_o = F_s/A \tag{2.4}$$

for an initial piston height of:

$$x_o = V_o/A \tag{2.5}$$

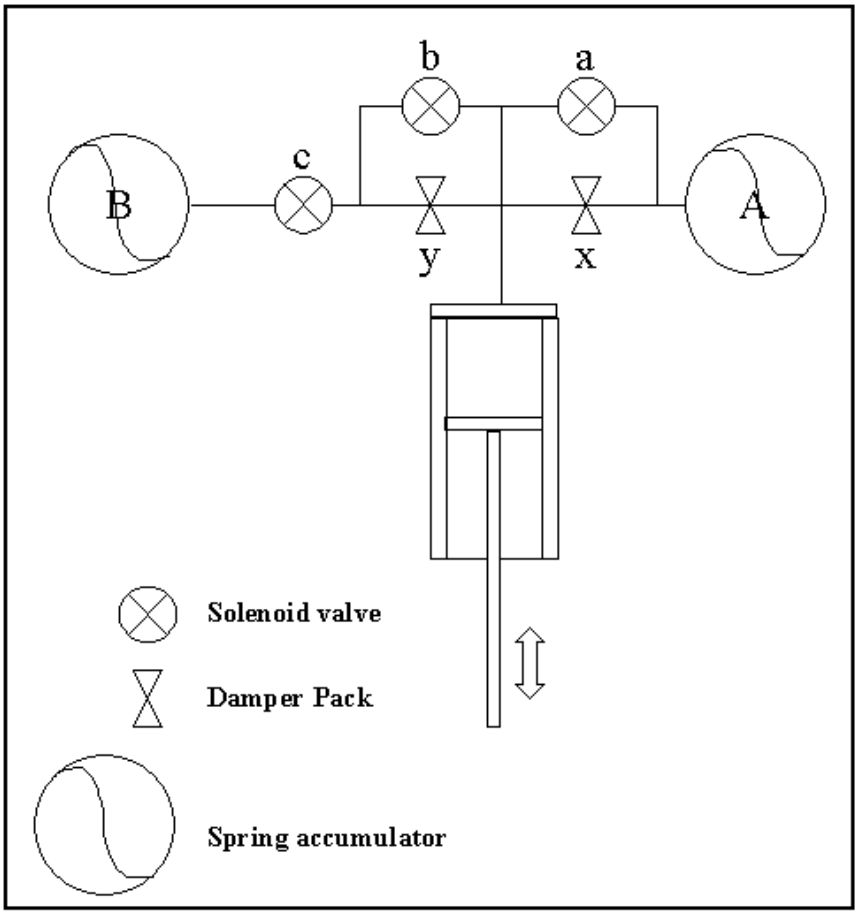

Figure 2.7: Schematic diagram of the hydro-pneumatic suspension unit

Table 2.1: Current spring force system design variables

Variable	Value	Name
x_s	316 mm	Static Spring Displacement
S	300 mm	Total strut stroke
Fs	5500 N	Static Spring load
R	25 mm	Accumulator piston radius
γ	1.3	Gas constant
V_o	1 liter	Static gas volume

and the ideal gas law constraint:

$$P_o V_o^{\gamma} = k \tag{2.6}$$

The current volume for the relative displacement x is defined as:

$$V = A(x_o + x) \tag{2.7}$$

with the current accumulator conditions also conforming to the ideal gas law constraint:

$$PV^{\gamma} = k \tag{2.8}$$

Thus using the current volume (equation 2.7) in equation 2.8 gives:

$$P(A(x_o + x))^{\gamma} = k \tag{2.9}$$

where the current pressure P can be defined in terms of the current force F_c as:

$$P = F_c/A \tag{2.10}$$

resulting in the current force:

$$F_c = \frac{Ak}{(A(x_o + x))^{\gamma}} \tag{2.11}$$

For ease of comparison this force is measured relative to the static force to give:

$$F = F_c - F_s = \frac{Ak}{(A(x_o + x))^{\gamma}} - F_s \tag{2.12}$$

Figure 2.8 illustrates the resulting spring force vs. displacement characteristics that can be achieved for various static gas volumes, zeroed around the static suspension height and static vertical load of the Land Rover test vehicle.

Damper Characteristics:

For damping, the suspension unit has two separate damper packs that can be designed for the required damping characteristics. These damper packs can be completely bypassed by the solenoid valves, when demanded by the vehicles operating conditions. Currently the damper packs are standard Land Rover Defender rear damper packs. However, one of the purposes of this study is to determine exactly what characteristics are required. A prototype unit, of the proposed suspension unit, was tested in the Sasol Laboratory (Figure 2.9), using a Schenck hydropulse actuator in the test rig designed for the testing of the prototype.

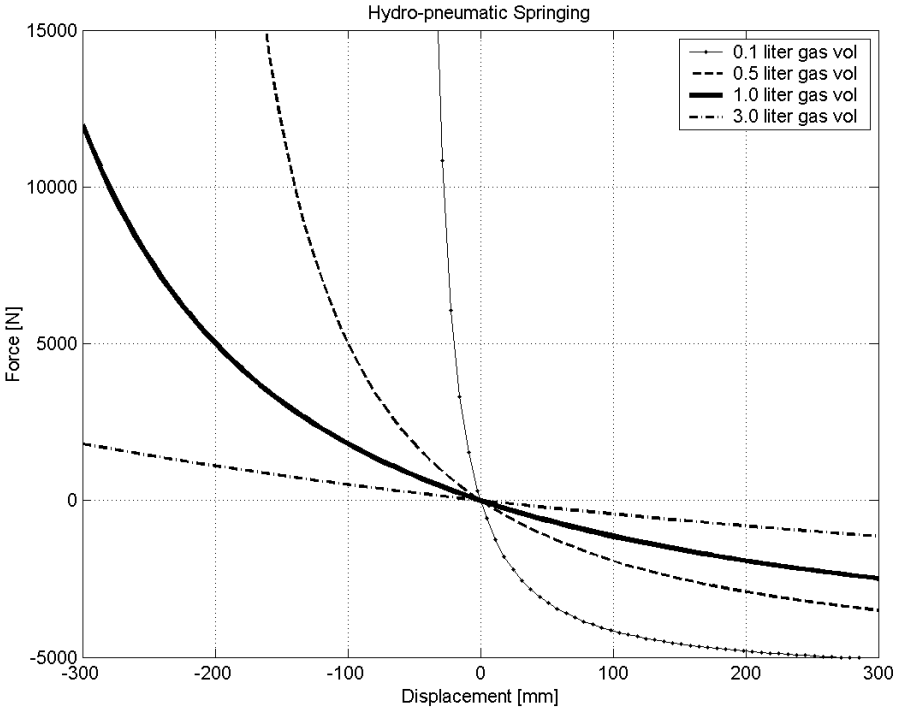

Figure 2.8: Hydro-pneumatic spring characteristics

2.1.4 Ride

The ride comfort of the vehicle depends on the motion of the whole vehicle and is a very subjective quantity, depending on the individual driver or passenger. Ride comfort is very important, as it is this characteristic that influences the potential purchaser of a vehicle. The ride comfort is defined in terms of the range of excitation frequencies between 0 and 25 Hz according to Gillespie [16], and 0 to 80 Hz according to the BS 6841 standard [17] and Reimpell and Stoll [18]. Noise is classified as frequencies above these levels. In this study, the emphasis is on ride comfort, rather than vehicle noise. The vehicles suspension system is the primary device used to minimize the discomfort, while engine vibration mounts and body materials generally affect the noise quality of a vehicle. There are many standards that relate to ride comfort measurement and acceptable levels of ride comfort of a vehicle [19, 17]. Different countries use different standards and measurement units. The most commonly used measurements are the frequency weighted RMS

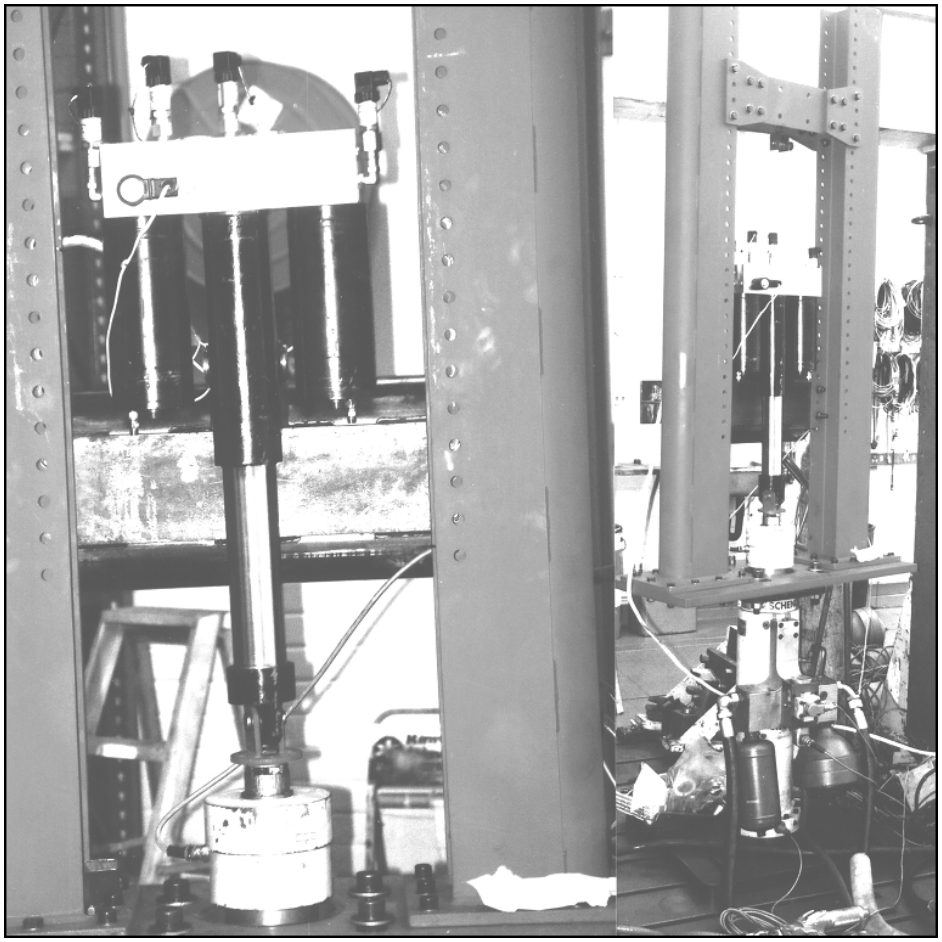

Figure 2.9: Hydro-pneumatic strut on test rig

acceleration, vibration dose value and average absorbed power.

The BS 6841 weighting curves for vertical ride comfort are illustrated in figure 2.10. The Root Mean Square (RMS) acceleration is defined as:

$$a_{RMS} = \sqrt{\frac{1}{T}\int_0^T a_w^2(t).dt} \tag{2.13}$$

with T being the total sample time, a_w the weighted acceleration, and t the time. For values of a_{RMS} above 1 m/s^2 the ride is rated as uncomfortable, and above 2.5 m/s^2 as extremely uncomfortable.

The vibration dose value is defined as:

$$VDV = \sqrt[4]{\int_0^T a_w^4(t).dt} \tag{2.14}$$

The vibration dose value takes the duration of the event into account and thus can only be compared with other events, if the same time span is taken

into consideration. Four hour VDV's with values above 16 $m/s^{1.75}$ are rated as uncomfortable, and above 26 $m/s^{1.75}$ as extremely uncomfortable. VDV also places more emphasis on the magnitude of the peaks of the acceleration in the frequency domain. The RMS acceleration and VDV are the most commonly used measures of ride comfort. The U.S.A. makes use of the Average Absorbed Power (AAP), where a value above 6 Watts is regarded as uncomfortable and above 12 Watts as extremely uncomfortable.

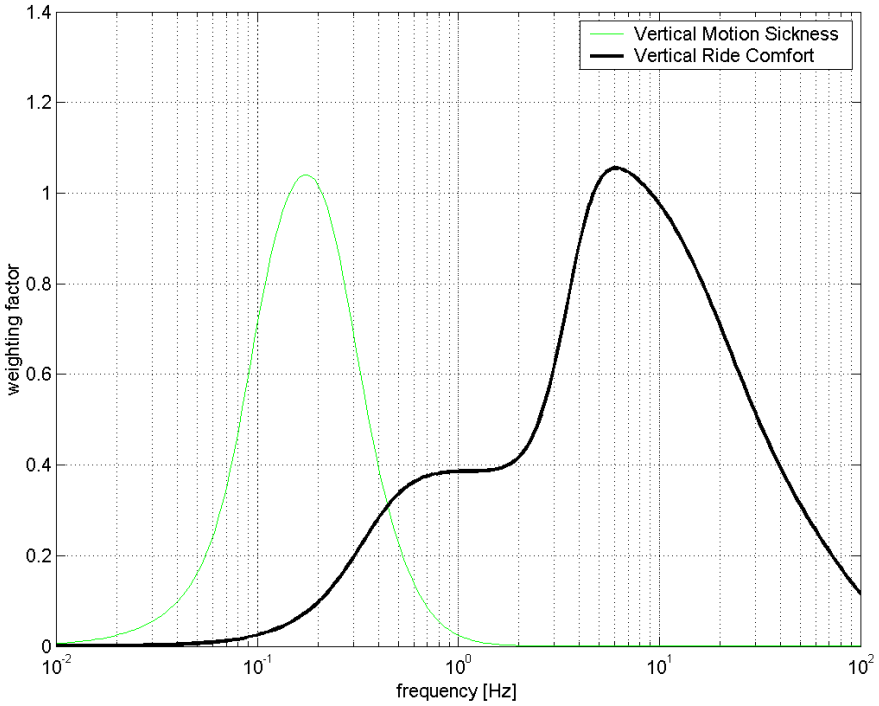

Figure 2.10: BS 6842 weighting curves for ride comfort

However, in a study conducted by Els [20] it was found that VDV and a_{RMS} exhibited a linear relationship between subjective and objective measurements, with AAP having a non-linear, but predictable, relationship between subjective and objective measurements. It was also found that the vertical acceleration values are of greater importance than the accelerations experienced in other directions by passengers. The conclusion reached is that the consistent application of one of the standards to vertical accelerations at the seat is sufficient for ride comfort evaluation. The BS 6841 weighted vertical acceleration is therefore used as the measure of ride comfort for the

optimisation of the spring-damper as discussed in Section 3.7.1.

2.1.5 Handling

The vehicle's suspension system is the main contributor to the vehicle's handling performance. The suspension kinematics, and dynamics, affect the vehicle's handling. The main focus of this study is on the effect of the dynamic elements (springs and dampers) on the vehicle's handling performance. Unlike ride comfort, no standard exists that provides the design engineer with guidelines, on the level of certain key parameters, that will provide good handling behaviour in a vehicle. This makes the definition of a handling objective function more challenging than for ride comfort. Many vehicle handling test manœuvres are used to measure vehicle handling. There are open loop manœuvres where the outcome of the manœuvre does not depend heavily on the driver-vehicle interaction. Typical manœuvres falling into this category are the steady state steering tests (constant radius, constant steer angle), and transient tests (J-Turn, Fishhook turn). There are also closed loop manœuvres that better describe real world handling manœuvres, such as the ISO 3888 [21] severe double lane change manœuvre that heavily depends on the driver-vehicle interaction. The important question that needs to be answered is : what measure must be used to evaluate handling? The results from a study (presented in Appendix A) indicate that there is a linear relationship between the lateral acceleration, body roll angle and yaw velocity.

Many researchers make use of yaw velocity gain as one of the measures of vehicle handling. The yaw velocity gain [16] is defined as the ratio of vehicle body yaw velocity Y_w to mean steering angle δ of the steered wheels, being:

$$G_{Y_w} = \frac{Y_w}{\delta} \tag{2.15}$$

The lateral acceleration gain [16] is defined as the ratio of vehicle lateral acceleration a_y to mean steering angle of the steered wheels, being:

$$G_{a_y} = \frac{a_y}{\delta} \tag{2.16}$$

Because of the linear relationship between the yaw velocity and lateral acceleration, these two gain values should exhibit a linear relationship as well. Crolla et al. [22] also observed that for transient cornering on a smooth road surface, the body roll angle correlates with the lateral acceleration phase, yaw velocity, lateral acceleration gain and yaw velocity gain. In studies conducted by Dahlberg [23] he states that:

> During steady state cornering on an even road under no influence of external forces, the level of lateral acceleration determines whether the vehicle rolls over or not.

Vehicle steering properties are normally tested by performing a constant radius test. From this the vehicle's speed and steering angle are compared. If the vehicle requires an increasing steering input as the vehicle speed increases, the vehicle exhibits under-steer. If the vehicle requires less steering input with increasing vehicle speed, the vehicle over-steers. If no steering adjustment is required with increasing vehicle speed, then it is a neutral-steer vehicle. The vehicle's spring stiffnesses can affect the steering behaviour of the vehicle. If the front roll stiffness is high (i.e. stiff springs in front), this induces under-steer characteristics, while a high rear roll stiffness will induce over-steer characteristics.

The vehicle body roll can result in an improvement in the vehicle's steering characteristics, refered to as roll-steer. This is especially true on trailing arm solid axle suspension systems, as in the Land Rover Defender. The trailing arm angle of the suspension at the rear, can result in over-steer, neutral-steer, or under-steer characteristics. If the trailing arm is horizontal with the ground, then it has a neutral-steer contribution. If the trailing arm is angled downwards, from the body to the rear axle, it has an over-steering contribution, as the inside wheel is pulled forward while the outside wheel is pushed outward in a corner. With an upward angle from the body to the axle, the trailing arm will have an under-steering effect, as with body roll the inside wheel is pushed outwards while the outside wheel is pushed forwards.

2.2 Optimisation Algorithms

Mathematical optimisation algorithms are being used more frequently in the product development phase, to obtain a more cost effective and improved design. There is an increasing amount of optimisation algorithms available to the designer. However, in spite of this proliferation of optimisation methods, there is no universal method for solving all possible optimisation problems. Each method seems to have its limitations. A short review of the optimisation algorithms applicable to this research is presented below.

Mathematical optimisation is the minimization of an objective function (design objective) subject to design constraints, in order to obtain an improved design configuration. The general optimisation problem, which optimisation algorithms aim to solve, is defined as:

$$\underset{w.r.t.\mathbf{x}}{^{minimize}} \quad f(\mathbf{x}), \quad \mathbf{x} = [x_1, x_2, .., x_n]^T \in R^n \tag{2.17}$$

subject to the inequality constraints:

$$g_j(\mathbf{x}) \leq 0, \qquad j = 1, 2, .., m \tag{2.18}$$

and the equality constraints:

$$h_j(\mathbf{x}) = 0, \qquad j = 1, 2, .., r \tag{2.19}$$

where $f(\mathbf{x})$, $g_j(\mathbf{x})$ and $h_j(\mathbf{x})$ are scalar functions of $\mathbf{x}$. In this formulation $\mathbf{x}$ is the vector of design variables, $f(\mathbf{x})$ is the objective function, $g_j(\mathbf{x})$ the inequality constraint functions, and $h_j(\mathbf{x})$ the equality constraint functions. The optimum solution is denoted by $\mathbf{x}^*$.

2.2.1 Gradient Approximation Methods

Most continuous optimisation methods require first order and/or second order gradient information of the objective and constraint functions with respect to the design variables. In most engineering optimisation problems this gradient information is not analytically available. The only information available to the designer is the values of the objective and constraint functions obtained via expensive simulations. The optimisation algorithm must

then approximate the gradients at each iteration step by using function values obtained from simulations. This is normally done by making use of finite differencing methods to approximate the gradient. The most common finite differencing method uses forward finite differences.

Forward Finite Difference (ffd)

This is the simplest and most economic method for approximating the gradients of the objective and constraint functions, required by gradient-based mathematical optimisation algorithms. This method approximates the first order gradient information of a multi-variable function $F(\mathbf{x})$, by evaluating the change in the function $F(\mathbf{x})$ for a small change dx_k in each of the design variables x_k, $k = 1, 2, ..., n$, as illustrated in Figure 2.11. Thus, in order to carry out the full gradient vector evaluation, a total number of $n + 1$ function evaluations are required for each iteration, where n is the total number of design variables. The forward finite difference approximation to the k^{th} component of the gradient at $\mathbf{x}$ is defined as follows:

$$\frac{\partial F}{\partial x_k} = \frac{F(x_1, x_2, ..., x_k + dx_k, ..., x_n) - F(\mathbf{x})}{dx_k} \tag{2.20}$$

for $k = 1, 2, ..., n$. Noisy objective functions, however, severely limit the accuracy of the forward finite difference gradient approximation, as is apparent from Figure 2.11. This can be partly overcome by using larger stepsizes dx_k or by considering instead, central finite differences.

Central Finite Difference (cfd)

This study also looks into the viability of using the central finite difference gradient evaluation procedure. Although this method requires $2n+1$ function evaluations per gradient vector evaluation, it may result in fewer optimisation iterations to obtain a minimum because of its greater accuracy. Central differences make use of a function evaluation on either side of the current iteration point $\mathbf{x}$, giving a more accurate approximation to the gradient of the underlying smooth function in the presence of noise. The central finite

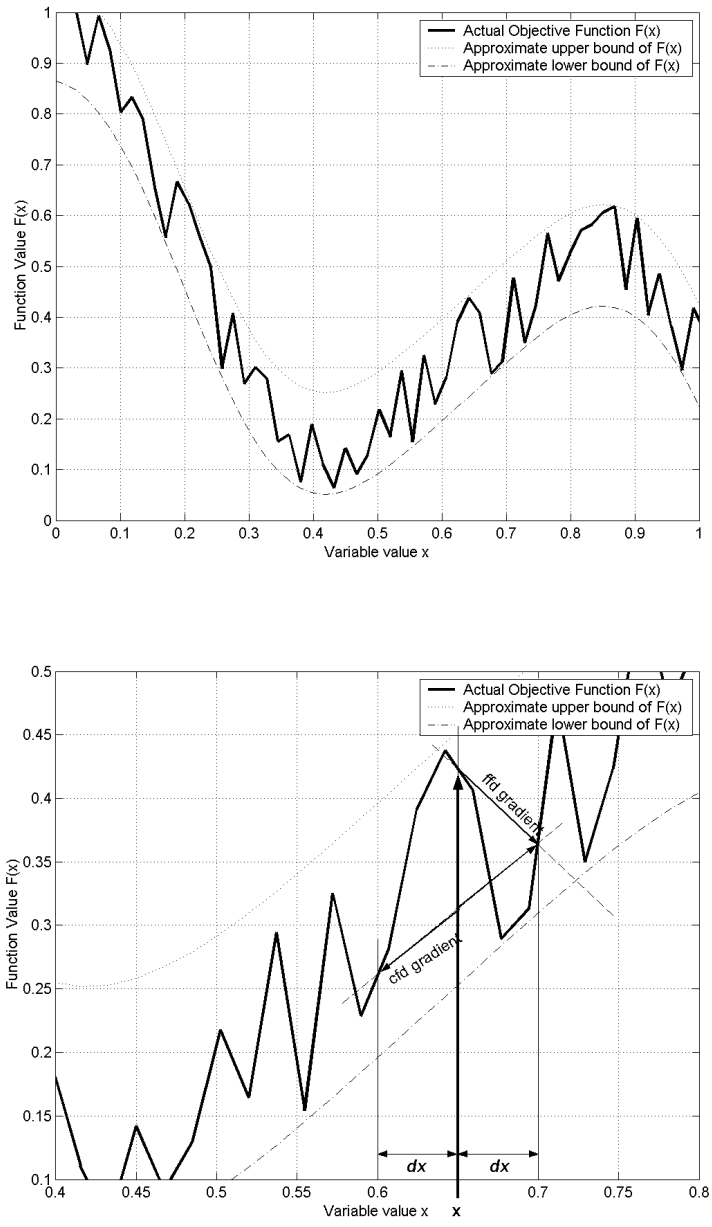

Figure 2.11: Finite difference gradient approximation methods

difference procedure is defined as follows:

$$\frac{\partial F}{\partial x_k} = \frac{F(x_1, x_2, ..., x_k + dx_k, ..., x_n) - F(x_1, x_2, ..., x_k - dx_k, ..., x_n)}{2dx_k} \quad (2.21)$$

for $k = 1, 2, ..., n$. In this way the gradient is evaluated by looking at what is happening behind and ahead of the current iteration point, while the forward finite difference only looks ahead of the current iteration point. Central differencing should therefore give a more accurate approximation to the function gradient as illustrated for the case depicted in Figure 2.11.

The effects of noise cannot be completely eliminated by this method, but it certainly yields gradient approximations that are superior to that given by forward finite differences. As can be deduced from Figure 2.11 the greater the perturbation dx_k, in the presence of noise, the more accurate the approximation of the gradient of the function becomes, no matter which finite differencing technique is used. However, too large a perturbation dx_k will result in the local optima being completely missed by the optimisation algorithm. Thus the correct selection of perturbations dx_k for the function at hand, is very important.

Second Order Curvature Approximation

The Sequential Quadratic Programming (SQP) method [25, 31] and other Quasi-Newton optimisation algorithms such as the Davidon-Fletcher-Powell (DFP) method uses, in addition to first order gradient approximations, also second order curvature information. This information is very costly to obtain, as it corresponds to a partial derivative of a partial derivative. This information is stored in a n x n square matrix, commonly known as the Hessian matrix. The Broyden-Fletcher-Goldfarb-Shanno (BFGS) approximation to the Hessian matrix is used in Matlab's implementation of SQP. The Hessian matrix is approximated and updated at iteration $k+1$, $k = 0, 1, 2, ...$ by:

$$H_{k+1} = H_k + \frac{\mathbf{q}_k \mathbf{q}_k^T}{\mathbf{q}_k^T \mathbf{s}_k} - \frac{H_k^T \mathbf{s}_k^T \mathbf{s}_k H_k}{\mathbf{s}_k^T H_k \mathbf{s}_k} \quad (2.22)$$

where

$$\mathbf{s}_k = \mathbf{x}_{k+1} - \mathbf{x}_k \quad (2.23)$$

and

$$\mathbf{q}_k = \nabla f(\mathbf{x}_{k+1}) - \nabla f(\mathbf{x}_k) \tag{2.24}$$

and

$$\nabla f(\mathbf{x}_k) = [\frac{\partial f}{\partial x_1}, \frac{\partial f}{\partial x_2}, ..., \frac{\partial f}{\partial x_n}] \tag{2.25}$$

At the start of the optimisation procedure, (i.e. at iteration $k = 0$) most algorithms set H_0 equal to any positive definite symmetric matrix, normally the identity matrix I. Thereafter the approximation is updated at every iteration via equations 2.22-2.25.

2.2.2 Sequential Quadratic Programming

The Sequential Quadratic Programming (SQP) optimisation algorithm mentioned above is considered the industry-standard method for constrained optimisation problems if the number of variables is not too large. The version used in this study is found in Matlab's Optimisation Toolbox [25]. It finds the solution by minimizing successive quadratic approximations of the objective function. The quadratic objective function of the sub-problem at iteration k, then takes on the form :

$$\underset{w.r.t.\mathbf{s}}{minimize} \quad F(\mathbf{s}) = f(\mathbf{x}_k) + \nabla^T f(\mathbf{x}_k)\mathbf{s} + \frac{1}{2}\mathbf{s}^T\mathbf{H}(\mathbf{x}_k)\mathbf{s} \tag{2.26}$$

where $\mathbf{s}$ is defined in terms of the next and current $\mathbf{x}$ values as:

$$\mathbf{x}_{k+1} = \mathbf{x}_k + \mathbf{s} \tag{2.27}$$

In constructing these approximations, second order curvature information is also required in the form of the Hessian matrix. The Hessian matrix is approximated by making use of the Broyden-Fletcher-Goldfarb-Shanno (BFGS) approximation described by equations 2.22-2.25. The Hessian matrix does require updating, which means an extra $n + 1$ function evaluations per iteration. The successive quadratic problems are solved iteratively for $\mathbf{s}$ until $\mathbf{s} = \mathbf{0}$. If an optimum of an approximate sub-problem lies outside the bounds, the violating variables are set to the boundary values. A line search is performed using $\mathbf{s}$ as the search direction, until a variable set is found that gives an objective function value equal to or less than the function value of

the previous iteration. For the line searching Matlab makes use of the merit function approach [26, 27].

2.2.3 Leap-Frog Algorithm LFOPC

The dynamic trajectory or Leap-Frog OPtimiser, LFOP, has been an ongoing development at the University of Pretoria since 1982 [28] when the first paper on this method was published. The approximation method Dynamic-Q [30], currently uses this method to solve spherical quadratic approximate sub-problems created at each iteration. In its current version Leap-Frog OPtimiser for Constrained problems, LFOPC [29], is designed to handle optimisation problems with constraints. The algorithm has the following characteristics :

- No explicit line searches are performed.
- No explicit function evaluations are required.
- Gradient information is the only explicit function information used.
- Two convergence tolerances and a maximum step size need to be specified.
- The algorithm is suitable for objective functions which exhibit noise.

The penalty function solution to the constrained problem is carried out in three phases.

- Phase 1 : Moderate penalty parameter value is used which gives fast and smooth progression to the region of $\mathbf{x}^*$.
- Phase 2 : A greatly increased penalty parameter is then applied to give a better approximation to $\mathbf{x}^*$, and the active constraints at this point are identified.
- Phase 3 : Determination of least squares solution of active set of constraints is carried out, with the shortest path from the phase 2 solution, to the actual $\mathbf{x}^*$ being taken.

LFOP Algorithm

The Leap-Frog OPtimiser (LFOP) for unconstrained optimisation is used for the optimisation of each phase in LFOPC. The algorithm seeks the minimum of a n variable function by considering the problem of the motion of a particle of unit mass in a n dimensional conservative force field. The potential energy of the particle is the function $f(\mathbf{x})$ to be minimized. The solution of the equations of motion of the particle, given an initial velocity and position, is required by the algorithm. The trajectory is approximated by using the leap-frog (Euler-forward-Euler-backward) method. An interfering strategy is applied to reduce the kinetic energy of the particle whenever it moves uphill. The particle is thus forced to follow the path to the local minimum $\mathbf{x}^*$. For more information on the algorithm the reader is refered to [28, 29, 30].

2.2.4 Dynamic-Q

The Dynamic-Q algorithm is defined as: 'Applying a *Dynamic* trajectory optimisation algorithm to successive spherical *Quadratic* approximations of the actual optimisation problem '[30]. This algorithm has the major advantage that it only needs to do relatively few function evaluations (simulations) of the original expensive objective and constraint functions to construct a simple quadratic approximate sub-problem. These approximate functions can then be cheaply evaluated and the optimum point of the approximate problem may be found economically, using the robust dynamic trajectory method LFOPC discussed in the previous sub-section. At this new approximate optimum point, new quadratic approximate objective and constraint functions are constructed, and the associated sub-problem solved. This procedure is iteratively repeated until convergence is obtained. This method is very efficient for optimisation problems with functions that require an expensive computer simulation for their evaluation. Dynamic-Q usually may make use of forward finite differences to obtain the gradient information required for the generation of the approximations. The basic details of the method are as set out below. A sequence of sub-problems $\boldsymbol{P}[i]$ $i = 0,1,2,\ldots$ is generated by

constructing successive spherically quadratic approximations to the objective and constraint functions, at successive points $\mathbf{x}_i$. The approximation to the objective function, for example, is as follows :

$$\tilde{f}(\mathbf{x}) = f(\mathbf{x}_i) + \nabla^T f(\mathbf{x}_i)(\mathbf{x} - \mathbf{x}_i) + \frac{1}{2}(\mathbf{x} - \mathbf{x}_i)^T \mathbf{A}(\mathbf{x} - \mathbf{x}_i) \tag{2.28}$$

The Hessian matrix $\mathbf{A}$ takes on a simple diagonal matrix form :

$$\mathbf{A} = a\mathbf{I}; \tag{2.29}$$

This form of Hessian matrices indicates that the approximate sub-problems are spherically quadratic in nature. The curvature a takes on a value of zero for the first sub-problem $i = 0$. Thereafter it is defined by :

$$a = \frac{2[f(\mathbf{x}_{i-1}) - f(\mathbf{x}_i) - \nabla^T f(\mathbf{x}_i)(\mathbf{x}_{i-1} - \mathbf{x}_i)]}{\|\mathbf{x}_{i-1} - \mathbf{x}_i\|^2} \tag{2.30}$$

The approximate constraint functions are constructed in a similar manner. If the gradient vectors ∇f, ∇g_j, and ∇h_j are not known analytically they may be approximated by first order finite differences.

Additional side constraints of the form $\hat{k}_i \leq x_i \leq \check{k}_i$ are normally imposed on the design variables. Because these constraints do not exhibit curvature properties they are treated as linear inequality constraints.

To obtain stable and controlled convergence of the solutions of successive sub-problems, a move limit is set which takes on the form of an inequality :

$$g_\delta(\mathbf{x}) = \|\mathbf{x} - \mathbf{x}_i\|^2 - \delta^2 \leq 0 \tag{2.31}$$

where δ corresponds to a specified move limit. The sub-problem at $\mathbf{x}_i$ can now be solved using the dynamic trajectory 'Leap-Frog' optimisation algorithm for constrained optimisation LFOPC. This solution is taken as $\mathbf{x}_i$, the point at which the next approximate sub-problem is constructed. This process is continued until convergence is obtained.

2.2.5 Genetic Algorithms

Genetic algorithms (GA's) do not use gradient information but rather perform stochastic searches of the design space in order to minimize the objective

function. The stochastic searching is, however, improved by the application of reproductive theory. The reproductive theory is implemented by the selection of the fittest members (possible solutions $\mathbf{x}_i$, $i = 1, 2, ..., N$) of the population (with N members) and allowing them to reproduce, mutate and crossover, creating a stronger population (lower objective function values) with time(iterations). The fact that no gradient information is required, is the main argument for the use of genetic algorithms. However, a substantially large population (N) is required to approach the minimum, if the design space is to be comprehensively covered. This results in the need to perform many function evaluations from the beginning. GA's are normally terminated on objective function value or variable changes are within tolerances. Because GA's do not require gradient information they fall into the class of zero-order optimisation algorithms together with the Nelder-Mead and simulated annealing methods.

2.2.6 Nelder-Mead

Nelder-Mead like the GA's is a zero-order optimisation algorithm. The main advantage of the Nelder-Mead [31] algorithm is that like genetic algorithms it does not require gradient information, and is easy to code, resulting in its more wide spread use. Because gradient information is not required, the Nelder-Mead algorithm is a good choice if the objective function has discontinuities over the design space. The Nelder-Mead, or simplex method as it is often called, creates a generalized triangle or simplex in n dimensions. The simplex points are evaluated with the point having the highest function value being replaced with a new point. With every iteration the size of the simplex is increased or reduced. The new point is normally reflected opposite to the poor point by the axis between the best two points. If the new point exhibits no improvement in the objective function value a new point is selected at twice the distance from the previous point. If this is still unsuccessful the worst point is replaced by one in the middle of the triangle. The points are again evaluated and the worst point is changed as before, until termination occurs. Termination normally occurs when the function value

or variable changes are within prescribed tolerances. Although this method was originally designed for unconstrained optimisation, the application of the penalty function process makes it possible to use it for constrained optimisation. The disadvantage with the Nelder-Mead optimisation procedure is that it is slower than most first order methods. As a result it requires many more function evaluations, resulting in a computationally more expensive method.

2.2.7 Sequential Linear Programming

Sequential linear programming uses linear approximations of the objective and constraint functions obtained from truncated Taylor series expansions. The inequality constraints are transformed to equality constraints. This is done as the optimum will lie on the boundary. Only the critical constraints are considered for the current iteration. These linear approximations are then cheaply solved for the minimum, subject to move limits imposed on the design variables. This then limits the variables to a gradual move towards the global optimum. The optimum will normally lie at the intersection of constraints. This point is then used for the linear approximation of the objective and constraint functions, for the next iteration. This process is continued iteratively until a minimum is found that conforms to the constraints and termination criteria.

2.3 Vehicle Suspension Optimisation

2.3.1 Scania Bus

Eriksson and Friberg [32] investigated the use of mathematical optimisation of the engine mounts of a city bus for ride comfort enhancement. The engine mounts were assumed to exhibit a linear characteristic for both spring and damper. There were thus two spring constants and two damper constants equating to a four design variable optimisation problem. The body of the bus was modelled as a flexible finite element method (FEM) model, with spring and damper characteristics assumed linear. A measured random road profile was inserted as the input to the four wheels. The normalised sum of

the weighted vertical accelerations at three points in the bus was used as the objective function. The optimisation algorithm used was the IDESIGN [33] recursive quadratic programming algorithm (similar to SQP). The results showed that convergence was achieved in 12 iterations using 63 function evaluations. The objective function exhibited a few local minima points, with an improvement of seven percent in the ride comfort being obtained. Eriksson stated [32] :

> A problem with the current gradient based algorithm is the result dependency on the choice of starting design.

Recently Andersson and Eriksson [34] presented a procedure for the optimisation of the handling and ride comfort of a bus. The ride comfort was again evaluated by observing the nature of the vertical accelerations in three positions in the bus, but also looked at the weighted vibration dose values (VDV) for the bus travelling over double and single sided obstacles in the road. For handling optimisation the bus performed a single lane change manœuvre at 80 and 40 km/h. They reported that the minimization of the maximum yaw velocity gain provides better optimisation results than the minimization of the minimum yaw velocity time lag, with a constraint on the maximum body roll angle, so as to ensure sufficient roll stiffness. Individual and combined optimisation was performed, and for the individual case an 18 percent improvement in ride comfort was obtained, while for the combined optimisation a 12 percent improvement was achieved. For the ride comfort optimisation it is stated that six out of the eight variables ran to their bounds. The built in Sequential Quadratic Programming method in ADAMS 12 [35] was used. The variables were the front and rear gas spring stiffnesses, front and rear anti-roll bar diameters, and the front and rear multiplication factors of the damper force for both compression and rebound.

2.3.2 Neural Network Approximation Approach

Gobbi et al. [36, 37, 38, 39] have done extensive work in the field of robust vehicle suspension optimisation. The models use linear characteristics for both

springs and dampers with up to as many as 38 design variables being considered for 38 performance indices describing both ride comfort and handling for ranging vehicle speeds [37]. The variables correspond to characteristics relating to tyre pressures, springs and dampers, rubber suspension bushes and bump stops. For such an extensive optimisation problem the vehicle multi-body dynamics model was used to train an artificial neural network (ANN) [36, 37]. The ANN makes use of 38 state equations and uses the back propagation method. The Spearman rank correlation coefficient [40, 41] was used to reduce the number of performance indices, by investigating correlations between indices. Multi-objective programming techniques have been employed for the description of the overall objective function. The ANN is then optimised using Genetic Algorithms. Separate ANN's have been trained for each prescribed manœuvre of the three dimensional vehicle model, taking about 1000 function evaluations per ANN trained. An overall mean error of less than 2 percent was achieved between ANN and the mathematical multi-body dynamics model, which was also correlated with experimental data.

2.3.3 LFOPC and Damper Optimisation

Naude and Snyman [12, 13] and Naude [14] made use of the LFOPC algorithm to optimise a six-wheeled military vehicle's ride comfort by using a six piece-wise linear damper characteristic. A problem specific program was written to enable speedy solution of the objective functions. The vehicle was modelled as a pitch plane model driving over a dirt road, Belgian paving and 200mm ditch bump profile. The objective function was the average of four vibration dose values. These are the vertical accelerations of the driver, the center of gravity, and a point at the rear, as well as the pitch acceleration of the vehicle body. The LFOPC algorithm required about 40 iterations to reach an optimum. This was acceptable since the custom written objective function evaluator required only a few seconds to perform the necessary function evaluations. The optimised damper characteristics took on a four piece-wise linear relationship. Of interest was the existence of many local minima of

the objective function that gave the same objective function value.

2.3.4 Dynamic-Q Two Variable Optimisation

Els and Uys [24] investigated the applicability of using the Dynamic-Q optimisation algorithm for the optimisation of a SUV's spring and damper characteristics. Only two variables, corresponding to the spring and damper characteristics, were used in the optimisation process. The spring variable is the static gas volume while the damper variable is a force multiplication factor for the damper characteristics. A full three dimensional DADS vehicle model was used in simulating driving over the Belgian paving and the driver's weighted vertical RMS acceleration was used as a measure of ride comfort. For handling the vehicle was simulated performing the double lane change manœuvre at 60 km/h, with the first peak value of the body roll angle being used as the objective function. The optimisation process was performed manually, and not integrated with the simulation program DADS. The combined optimisation of the vehicle performing the double lane change over the Belgian paving was also performed with promising results.

2.3.5 SLP and Damper Optimisation

Etman et al. [11] proposed the optimisation of a stroke dependent damper characteristic for the front suspension of a truck using Sequential Linear Programming (SLP) with a move limit strategy. The goal was to achieve the best compromise between the suspension system's working space and driver comfort. First a quarter car model was considered for the optimisation, thereafter a full three dimensional model of the truck and semi-trailer was built. The damper characteristics were described in terms of the empirical relationship proposed by Etman et al. and discussed earlier in Section 2.1.3. Three road disturbances were considered, namely a 250mm traffic hump, 500mm sine wave hump, and a typical railway crossing. It was found that consideration of the wave and hump were the critical road conditions with regards to finding an acceptable design. It was found that multiple local minima of the objective function occurred. For the three dimensional model

the following simplifications were carried out:

- The bump stops were not modelled, as contact with the bump stops, leads to a series of high frequency accelerations that makes numerical computation expensive.
- The vehicle makes contact with the obstacles with both front tyres at exactly the same time.
- Design variables found to run to their bounds for the quarter car analysis, were kept at their respective bounds.

Etman et al. concluded that the shape of the damper curve was very dependent on the vertical accelerations. They proposed the following design rules:

> The blow-off stiffness can remain small. The bleed and blow-off pre-load are important variables. To reduce inward suspension deflection, the compression side of the damping curve is of main interest.

They express concern about the large step taken in progressing from a quarter car model to full scale vehicle model, and point out the necessity of a model of intermediate complexity for optimisation. Such an intermediate model was constructed and optimised by Naude [12]. Also, some difficulties in the full scale optimisation were attributed to inaccurate finite difference gradient approximations, and a multi point finite difference approach is suggested.

2.3.6 SQP and Damper Optimisation

Eberhard et al. [10] made use of a pitch plane vehicle model to optimise for driver comfort and safe driving over a single obstacle. The weighted vertical acceleration was used as a measure of comfort, and the normalised tyre vertical force as a measure of safety. The nonlinear damper characteristics were modelled by Hermite splines as described earlier in Section 2.1.3. The Sequential Quadratic Programming (SQP) algorithm was used for the optimisation. Eberhard et al. conclude that the Hermite splines were difficult to

implement and required substantial user input, also that the problem should be expanded to two dimensional damper characteristics where velocity and displacement are taken into account.

2.3.7 BMW Vehicle Optimisation Procedure

Schuller et al. [42] proposed modelling of the vehicle components and behaviour by making use of transfer functions in a Simulink environment. This allows the vehicle model to be evaluated faster than real-time. A total of 150 design variables are considered, where the suspension dynamics and kinematics are described by non-linear characteristic curves. These curves are approximated using Hermite splines, where the design variables are the coefficients of the splines. For handling, only open loop manœuvres were considered, being the J-Turn and steady-state constant radius test. Many measures were used for the handling objective function, some being peak lateral acceleration, maximum body roll angle, yaw velocity gain, and yaw response time. The ISO 15037 [43] rough road test was used for the ride comfort manœuvre. The vehicle's center of gravity (cg) deviation from the straight path, the vertical RMS deviation of the vehicle body from the design level, and the maximum yaw velocity were used as the ride comfort objective function. Genetic Algorithms were used for the multi criteria optimisation, with improvements achieved over the baseline vehicle in all manœuvres. Only side constraints were set on the design variables, being 50 percent change from the baseline vehicle, with no consideration made for feasibility of the optimised design in terms of kinematics. The most significant changes suggested by the optimisation study, were to increase the mass of the vehicle body and wheelbase, while decreasing the yaw moment of inertia. Schuller et al. [42] stated that the integration of a driver model in the optimisation procedure, enabling closed loop manœuvres, would lead to:

> a new quality in the optimisation of vehicle handling behaviour in simulation.

3. THE OPTIMISATION PROBLEM

3.1 Problem Statement

The optimisation of the spring and damper characteristics of a Land Rover Defender 110 Wagon, for ride comfort and handling, is to be investigated. The vehicle is fitted with the semi-active hydro-pneumatic suspension unit, described in Section 2.1.3.

3.2 Introduction

Because of the increasing use of SUV's and the current research focus at the University of Pretoria on suspension systems, a Land Rover Defender 110 Wagon is being investigated for the application of the semi-active hydro-pneumatic suspension system. The suspension has to be tuned for the appropriate spring and damper characteristics for all road conditions. The suspension characteristics will therefore be optimised for both ride comfort and handling.

The published works on vehicle suspension optimisation, described in Section 2.3, all concentrate on the use of only one gradient-based optimisation algorithm, namely the SQP method, or GA's, without benchmarking against other algorithms. In a few studies [44, 45, 46] gradient-based algorithms, like SQP, have been compared to the performance of stochastic methods, like GA's. These studies, however, make use of a simplified pitch plane model to describe the dynamics. The stochastic methods, were found to be very expensive in terms of number of function evaluations. This study aims to provide the reader with more information regarding the use of the Dynamic-Q algorithm, as an alternative to the well-established and industry-standard gradient based SQP method.

3.3 Mathematical Model of Vehicle

3.3.1 General Background

A model of the Land Rover Defender 110 Wagon was built using the multi-body dynamics package ADAMS View [47], based on measurements of the vehicle's hard points. The model was made as simple as possible, while complex enough to realistically model the essential features.

The vehicle model consists of 23 rigid bodies excluding ground, 11 revolute joints, 10 spherical joints, 9 Hooke's joints, and one driving motion. This represents a system with 16 degrees of freedom (Table 3.1). The vehicle in question has leading arms, and a Panhard rod in front with trailing arms, an A-arm, and an anti-roll bar fitted to the rear suspension. A simplified steering system was also modelled to enable steering of the vehicle during handling simulations.

Table 3.1: ADAMS model degrees of freedom

Body	Degrees of Freedom	Associated Motions
Vehicle Body	6	longitudinal lateral vertical roll pitch yaw
Front axle	2	vertical roll
Rear axle	2	vertical roll
Tyres	4	rotation
Anti-Roll Bar	2	rotation (2x)
	Total	16

3.3.2 Vehicle Body

The vehicle body and chassis are assumed to be one rigid body with a specified mass and inertia. The inertias are obtained by scaling down data available for an armoured prototype Land Rover 110 Wagon, to correspond to our vehicle's lighter weight. These values are considered to be sufficiently representative.

3.3.3 Front Suspension

The front suspension (as schematically shown in Figure 3.1, and modelled in Figure 3.2) consists of 11 rigid bodies, and 14 joints, as detailed in Table 3.2. Suspension links that appear similar to spherical-spherical joints on the vehicle, are modelled by a connecting body, a spherical and Hooke's joint (Figures 3.1 and 3.2). This was required to prevent unnecessary instability that may arise when solving for the motion of a rotating link. On the actual vehicle, friction in the suspension joints prevents the suspension links from rotating. In the ADAMS model it is very inefficient, from a solution point of view, to include joint friction. Adding joint friction results in more degrees of freedom, as well as additional spring and damper connection forces. This results in longer solution times. The solution of the kinematic constraints is much faster than dynamic constraints. The inclusion of these bushing stiffnesses add unnecessary high frequency (noise) accelerations to the solution. As this study is only concerned with the ride comfort and not the noise aspect of the vehicle, all joints are modelled as kinematic constraints. An additional body has to be added to prevent the suspension from rolling forward with the vehicle. This was done to keep the model simple and to avoid modelling of joint friction. The prop-shaft connections to the axle are not modelled directly, although such modelling would have eliminated the need for the additional link that was introduced in the current model. The front suspension has four resulting degrees of freedom, being roll, vertical freedom, and two rotational degrees of freedom associated with the tyres.

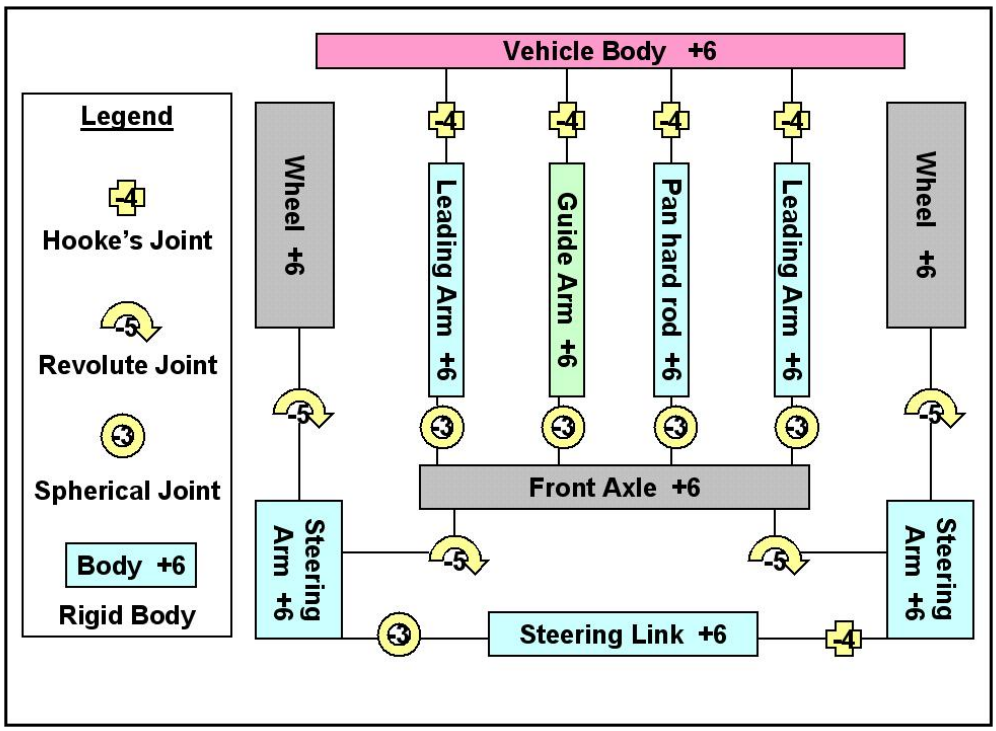

Figure 3.1: Land Rover front suspension schematic diagram

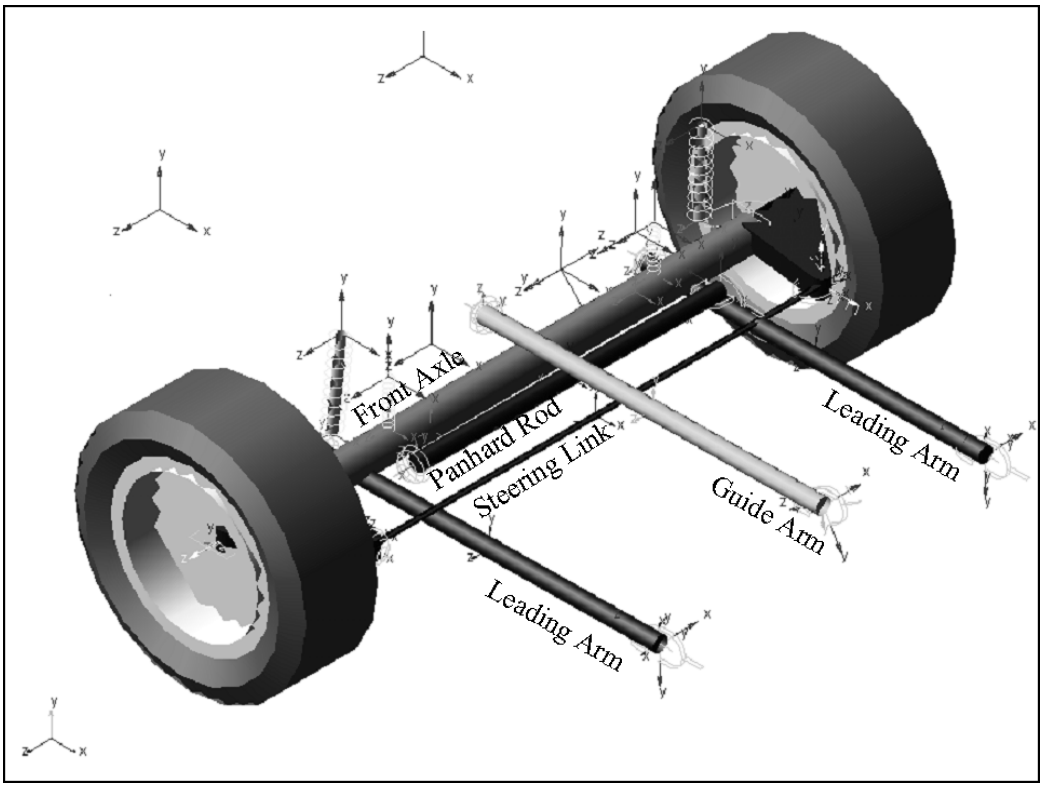

Figure 3.2: Land Rover front suspension modelling

Table 3.2: Front suspension model degrees of freedom

Quantity	Body	Degrees of Freedom	Result
	Rigid Bodies		
1	Front Axle	6	6
2	Leading Arms	6	12
1	Guide Arm	6	6
2	Wheels	6	12
1	Panhard rod	6	6
2	Steering Arm	6	12
1	Steering Link	6	6
		Sub Total	60
	Joints		
5	Hooke's	-4	-20
5	Spherical	-3	-15
4	Revolute	-5	-20
		Sub total	-55
	Motions		
1	Steering driver	-1	-1
		Total	4
1		Vertical	
1		Roll	
2	Wheels	Rotation	

3.3.4 Rear Suspension

The rear suspension (as schematically shown in Figure 3.3, and modelled in Figure 3.4) consists of 4 rigid bodies, 2 revolute, 3 spherical, and 2 Hooke's joints, detailed in Table 3.3. The suspension is a live axle with two trailing arms at the bottom, and one A-arm above the rear axle (Figure 3.4). The springs are mounted vertically to the body, but the separate dampers are at a trailing angle between the body and rear axle. The A-arm is modelled

using a rigid link with revolute and spherical joints at the ends. The trailing arms are modelled with a combination of Hooke's and spherical joints. The rear suspension has four resulting degrees of freedom, being roll, vertical translation, and two rotational degrees of freedom associated with the tyres.

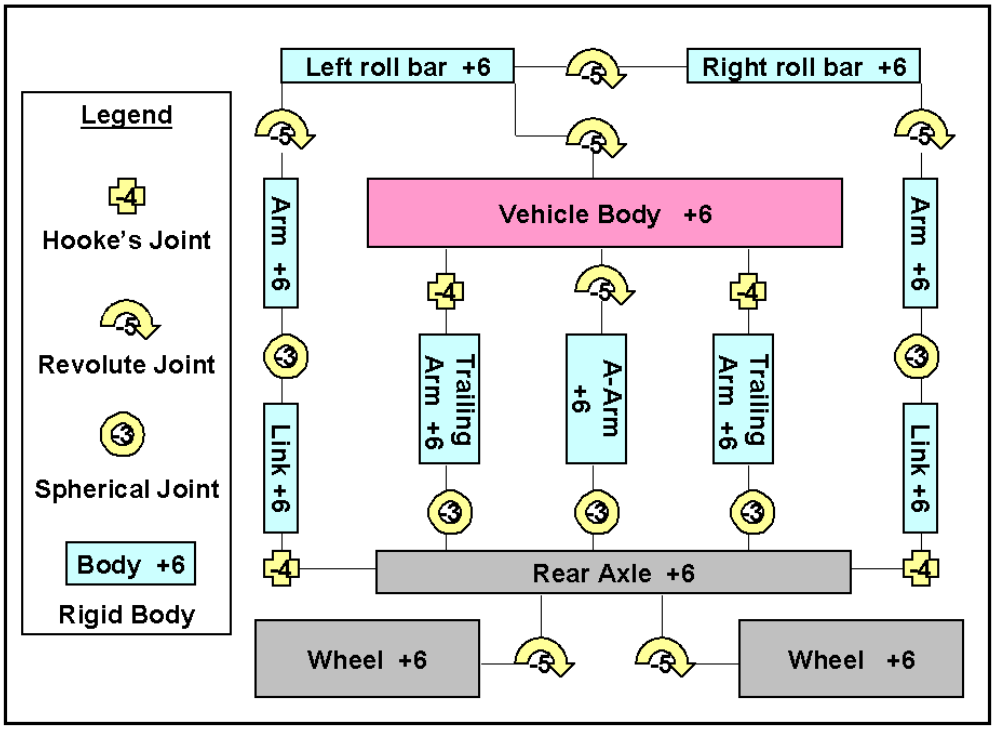

Figure 3.3: Land Rover rear suspension schematic diagram

3.3.5 *Anti-Roll Bar*

Attached to the rear suspension is the anti-roll bar system modelled with 6 rigid bars, 4 revolute, 2 spherical , and 2 Hooke's joints (Figure 3.3). The two bars at the rear are connected with a torsion spring with a stiffness of 22Nm/degree, which was determined from a finite element model of the anti-roll bar by Stipinovich [48]. These bars are connected to each other and the body by two revolute joints. Each of these bars are then connected to two side link bars, and the rear axle with one revolute, one spherical and one Hooke's joint (Figure 3.4). The rear anti-roll bar has two resulting rotational degrees of freedom, being the rotation of the rear bars in relation to the

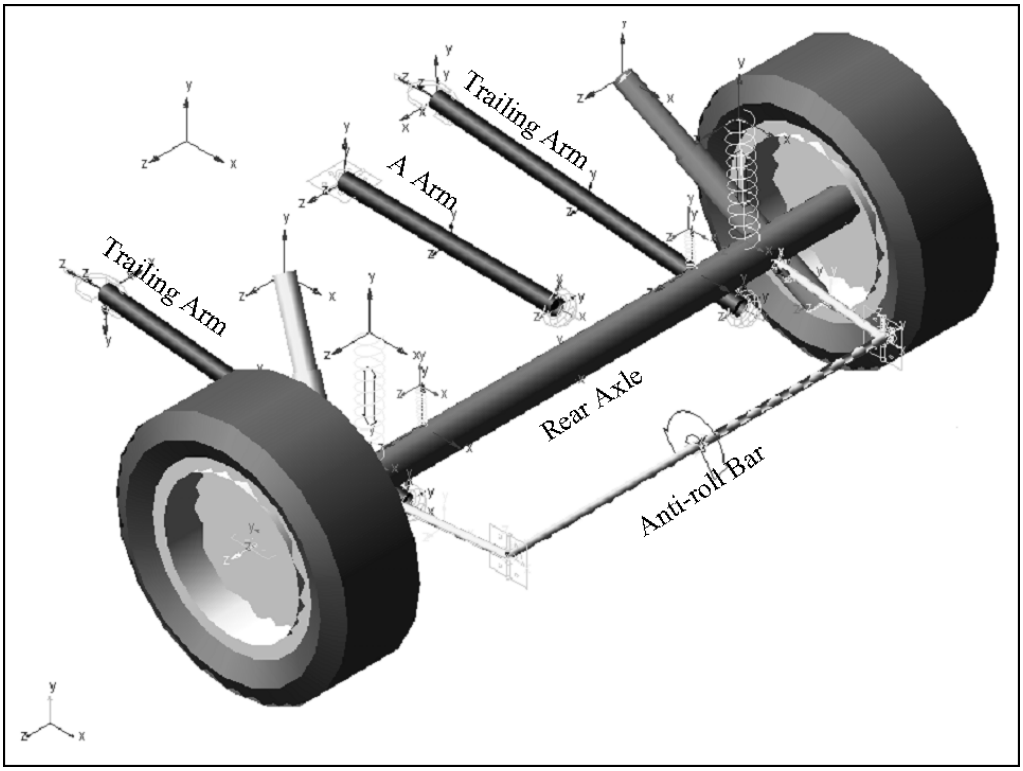

Figure 3.4: Land Rover rear suspension modelling

vehicle body.

3.3.6 Force Elements

The springs and dampers were first modelled using the standard ADAMS spring/damper element with a spline for force versus displacement and velocity. The new hydro-pneumatic suspension strut was modelled as a force between the two moving bodies. The gas spring characteristics were calculated in Matlab and imported as a spline into ADAMS. The displacement axis was scaled for the gas volume. This entails the multiplication of the axes by the gas volume. The damper characteristics are modelled by the non-linear function of 8 variables defining switch points and slope. An effort was made to fit the function proposed by Etman et al. to these characteristics [11]. This function, however, proved to be very difficult to fit to our current damper data, thus making the function non-viable. The details of the function are discussed in Section 2.1.3. For the initial investigation the rear damper graph was used and the force scaled with a design variable.

Table 3.3: Rear suspension model degrees of freedom

Quantity	Body	Degrees of Freedom	Result
	Rigid Bodies		
1	Rear Axle	6	6
1	A Arm	6	6
2	Trailing Arms	6	12
2	Wheels	6	12
2	Anti-roll Bar	6	12
2	Anti-roll Bar arms	6	12
2	Anti-roll Bar links	6	12
		Sub Total	72
	Joints		
4	Hooke's	-4	-16
5	Spherical	-3	-15
7	Revolute	-5	-35
		Sub Total	-66
		Total	6
1		Vertical	
1		Roll	
2	Wheels	Rotation	
2	Anti-roll Bar	Rotation	

3.3.7 Tyres

The tyres were created using the built-in ADAMS tyre module. Initially a Fiala tyre was selected because of its simplicity, and ADAMS license constraints. It was, however, found that the correlation with measurements could be improved if a load sensitive tyre was used. The 521 tyre was used for the handling and ride comfort simulations. This tyre is a simple lookup table interpolation tyre element for side-force and self-aligning torque, with ride comfort evaluated by a point follower model. Tyre data (Figure 3.5)

from tests conducted by LMT is used in the 521 interpolate tyre model. The four tyres are connected to the front and rear suspensions with revolute joints.

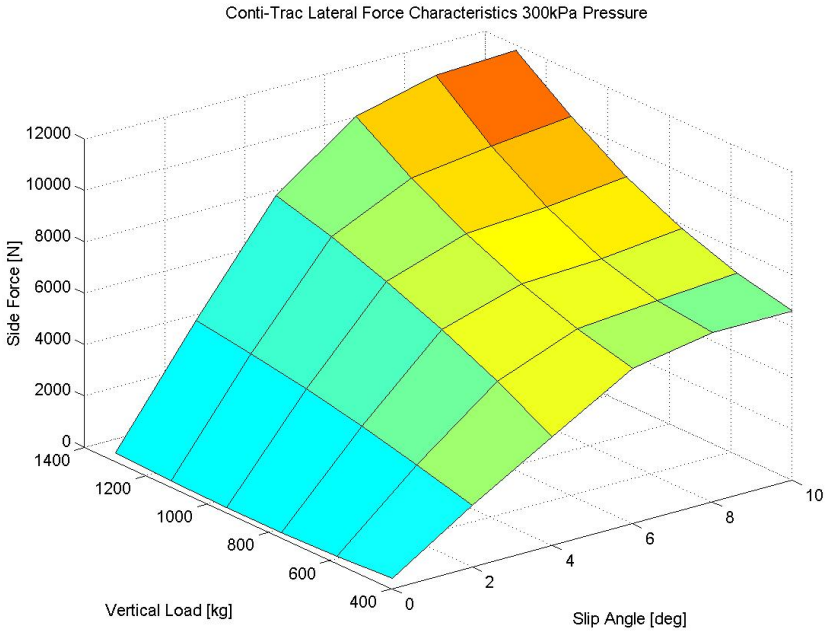

Figure 3.5: Tyre side force properties

3.3.8 Driver Implementation

For the vehicle to follow a specified path, a driver must be implemented. The steering driver implemented uses a marker at a preview distance in front of the vehicle (Figure 3.6) and adjusts the error according to the desired path to be travelled. This distance in front of the vehicle is defined as the driver preview distance, which can be calculated by multiplying the speed with the driver preview time. The differential equation describing the drivers action [49] with time t is:

$$\tau\dot{\delta}(t) + \delta(t) = -K \cdot d \tag{3.1}$$

where τ is the driver preview time:

$$\tau = \frac{l}{s} \tag{3.2}$$

with l the driver preview distance, s the vehicle speed, d the error, $\delta(t)$ the steering angle, and K the steering angle gain.

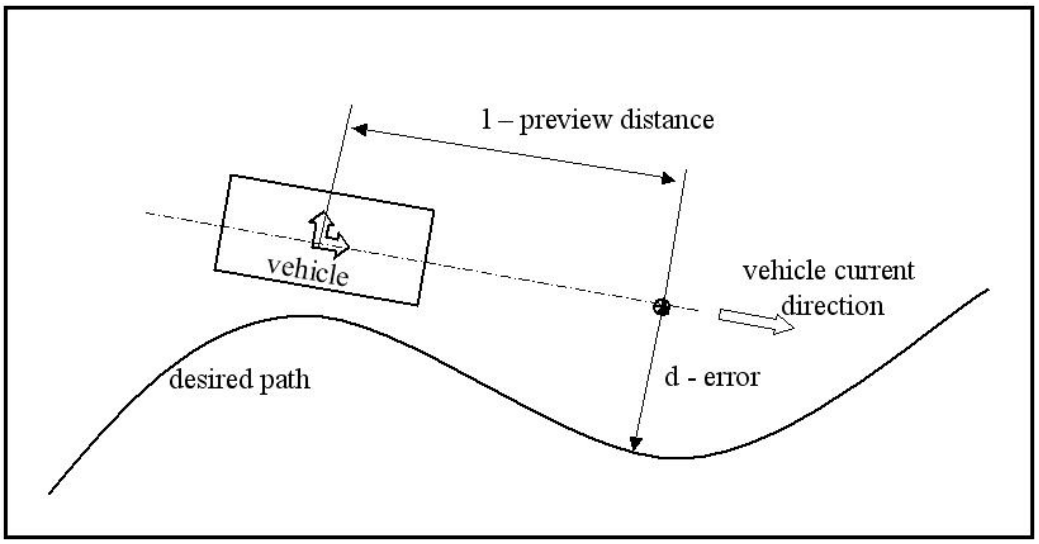

Figure 3.6: Implementation of driver model

For the vehicle to maintain a constant speed throughout the simulation, a speed driver must be implemented. A torque and force are applied to the wheels to ensure that the vehicle keeps a constant speed. This forcing value is calculated from the difference between the desired speed and actual vehicle speed, multiplied by a gain. Fifty percent of the force is applied as a horizontal force at the wheel centre, and the other 50 percent, multiplied by the wheel radius, as a torque on the wheel. The complete force was not added to the wheel as a torque, due to difficulties that were encountered, associated with the longitudinal dynamics of the tyre. The ratio used was found to be a good compromise. This is permitted, as this research is not concerned with the longitudinal dynamics of the vehicle, but rather the lateral dynamics (handling) and the vertical dynamics (ride comfort). With the full vehicle model illustrated in Figure 3.7.

3.4 Model Validation

Every mathematical model needs to be evaluated for accuracy against measured test data. A Land Rover Defender 110 Wagon was fitted with test

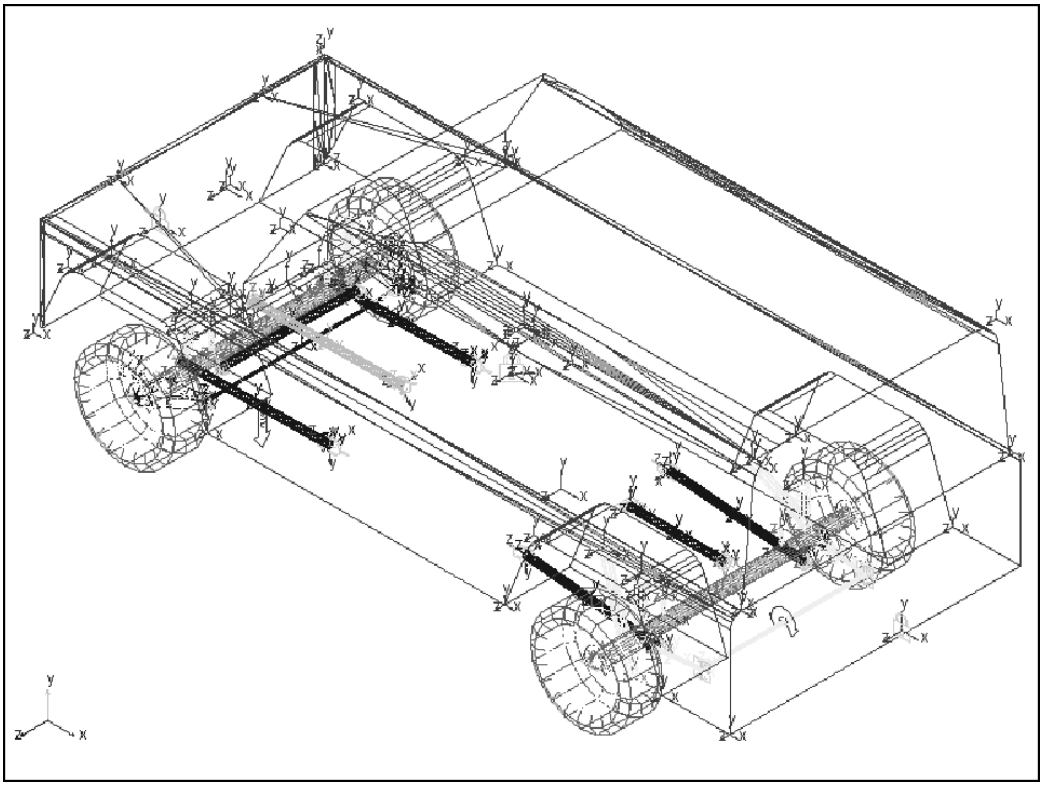

Figure 3.7: Full Land Rover model

equipment as described in Table 3.4 and illustrated in Figure 3.8. The vehicle then performed the double lane change manœuvre at 80 km/h, with half crew (2340 kg) and fully laden (2640 kg). Then it drove over the local Aberdeen Proving Grounds (apg) 100mm bumps at various speeds, and also crossed the Belgian paving at various speeds. The results for the comparison between the ADAMS model and the measured results for the apg are presented in Figure 3.9. Good agreement between the measured results and the ADAMS model were achieved. In Figure 3.10 the results for the vehicle performing the double lane change manœuvre at 80 km/h are presented. Although the handling agreement of the measured and the ADAMS model results is acceptable, for the purpose of the current study, the agreement is not as good as for the vertical dynamics. This is attributed to the single point preview driver model used in this study for the execution of the double lane change. It was suggested [50] that a three-point preview controller would perform better at executing the double lane change manœuvre than a single point preview controller. This, however, is still not the ideal driver model

for transient closed loop manœuvres. The three-point preview controller was recently implemented and found to be much smoother. The original single point controller model was, however, used consistently throughout this research. As can be seen from Figure 3.10 the steering input provided by the driver model contains more high frequency corrections than the measured steering response. This results in the very noisy nature of the front lateral acceleration. The rear lateral acceleration is much cleaner than the front lateral acceleration. This is attributed to the smaller influence the steering input has on the rear of the vehicle. This research, however, only uses the first four seconds of the simulated data of the double lane change manœuvre, which is in reasonable agreement with the measured results, of the same order of magnitude, and exhibits the same tendencies.

Table 3.4: Land Rover 110 test points

channel	point	position	measure	axis
1	B	center of gravity	velocity	longitudinal
2	G	left front bumper	acceleration	longitudinal
3				lateral
4				vertical
5	C	rear passenger	acceleration	longitudinal
6				lateral
7				vertical
8	I	right front bumper	acceleration	vertical
9	A	steering arm	displacement	relative arm/body
10	D	left rear spring	displacement	relative body/axle
11	E	right rear spring		
12	F	left front spring		
13	H	right front spring		
14	B	center of gravity	angular velocity	roll
15				pitch
16				yaw

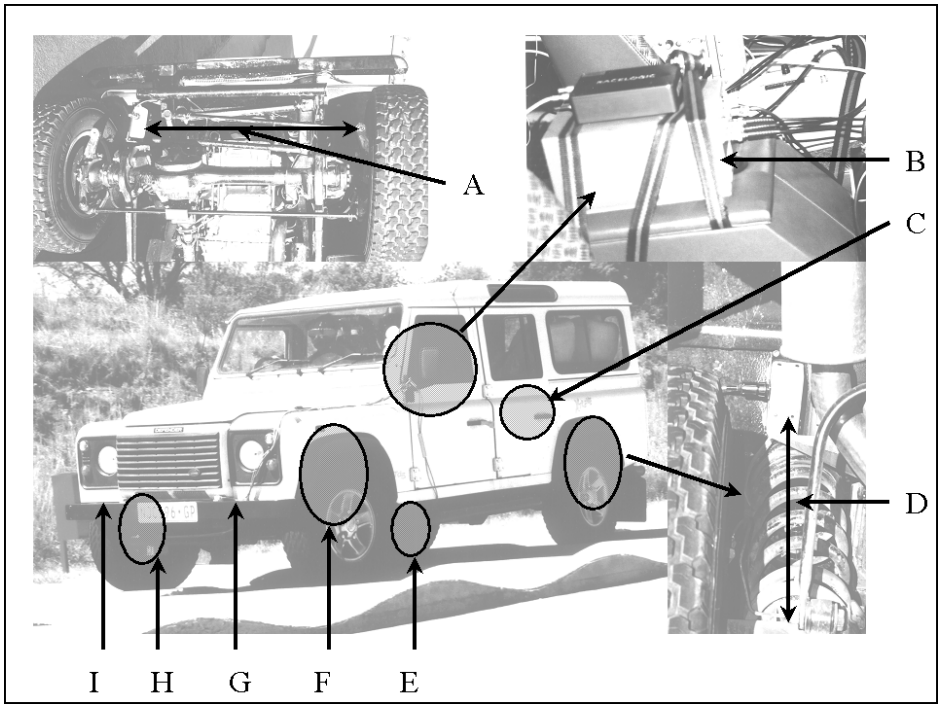

Figure 3.8: Test vehicle indicating measurement positions

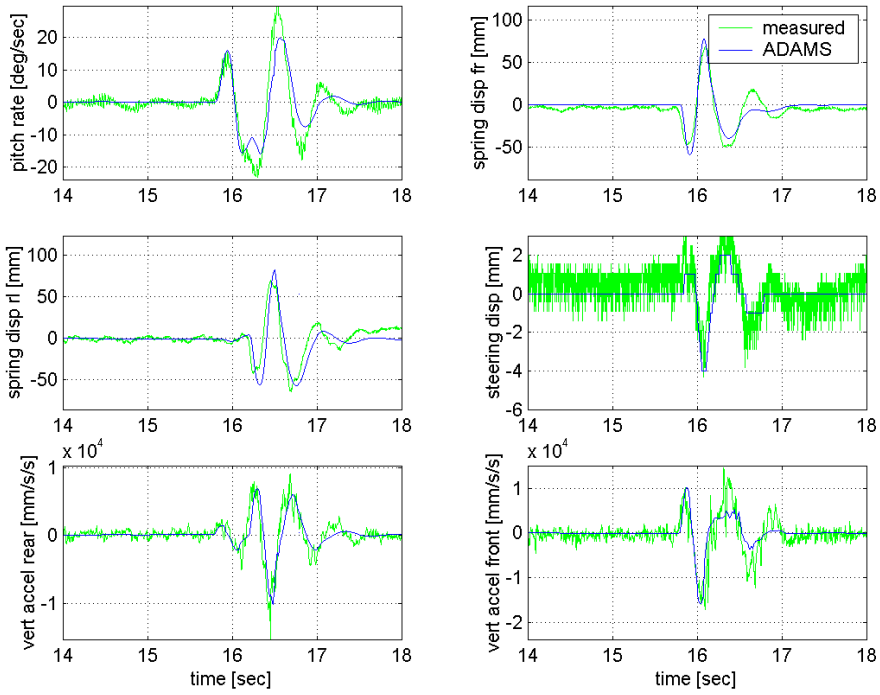

Figure 3.9: apg, 25km/h, Model validation results

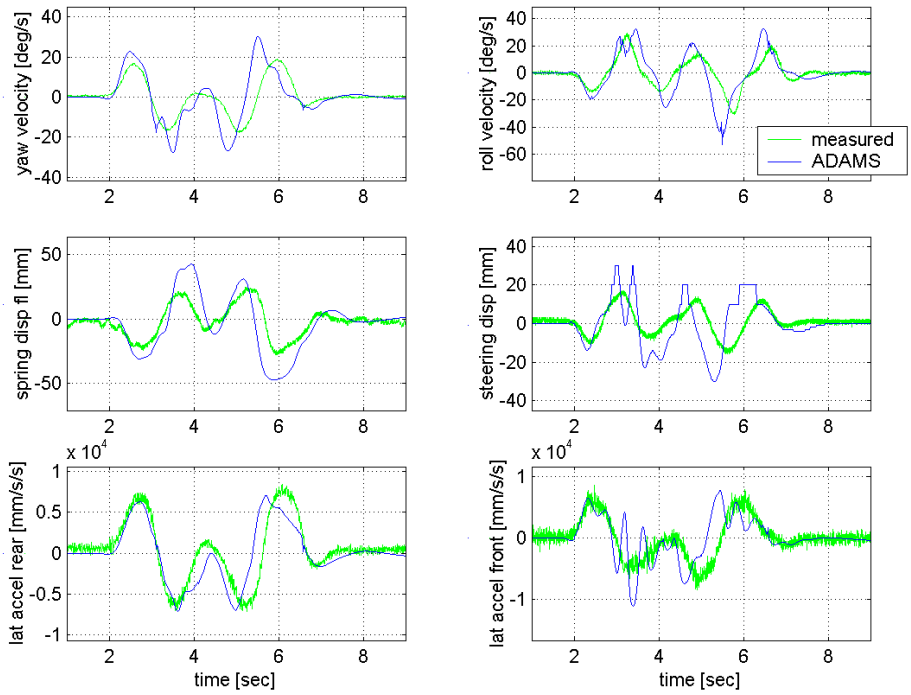

Figure 3.10: Double lane change, 80 km/h, model validation results

3.5 Optimisation Algorithms

The optimisation algorithms chosen for this investigation are the Dynamic-Q method and the industry-standard SQP method. The SQP method is chosen because of its wide acceptance as a superior optimisation method. The Matlab implementation of SQP was preferred to the built-in ADAMS SQP. As the model had to be made compatible with Matlab, this provided an easy comparison of results. Also ADAMS has a new SQP algorithm available in the latest version that makes future comparisons difficult, as the user does not know what the next built-in optimisation algorithm will be. This is due to uncertainties as to license agreements between the optimisation company and Mechanical Dynamics. The University of Pretoria currently has a licence for the Matlab optimisation toolbox, making it more convenient for future comparison purposes.

The Dynamic-Q method was selected for its proven applicability to suspension design [24], and in the solution of computational fluid dynamics

problems [51, 52, 53]. These problems exhibit noise and discontinuities for which Dynamic-Q appears to be suitable. Naude [14] also suggests in his thesis that the coupling of Dynamic-Q to a multi-body simulation package should be considered for future work.

3.6 Design Variables

In choosing the design variables for optimisation, the assumption is made that the left hand and right hand suspension settings will be the same, but that front and rear settings may differ. The design variables chosen for optimisation are therefore the static gas volume (Figure 3.11), and damper scale factors (Figure 3.12), on both the front and rear axles.

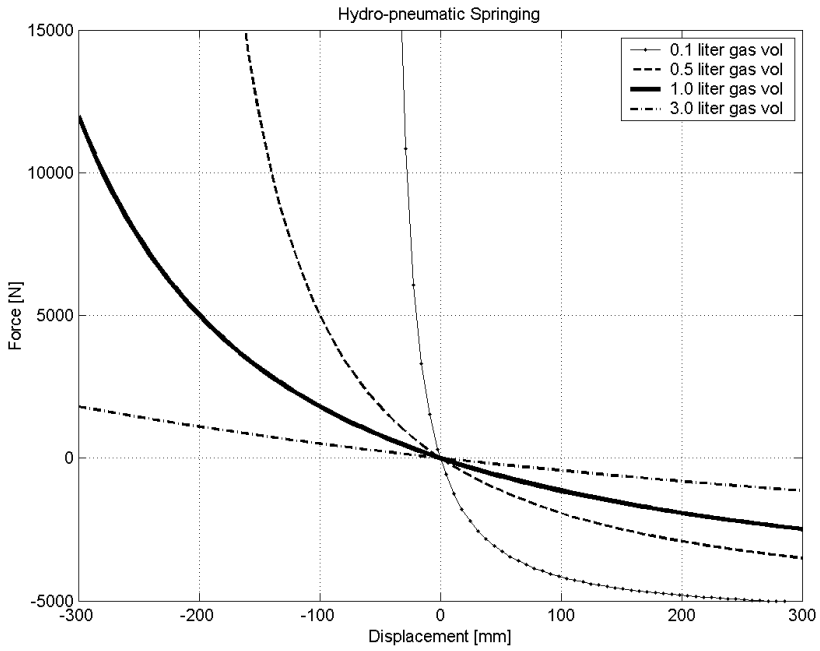

Figure 3.11: Definition of spring characteristics for various gas volumes

For the initial study the standard damper force characteristic is multiplied by a factor which constitutes the damping design variable (Figure 3.12). The general shape and switch velocities of the damper are thus kept the same. This research considers the cases of two and four design variables, which respectively corresponds to the cases where the spring and damper characteristics are identical for the front and rear axles (two design variables), and

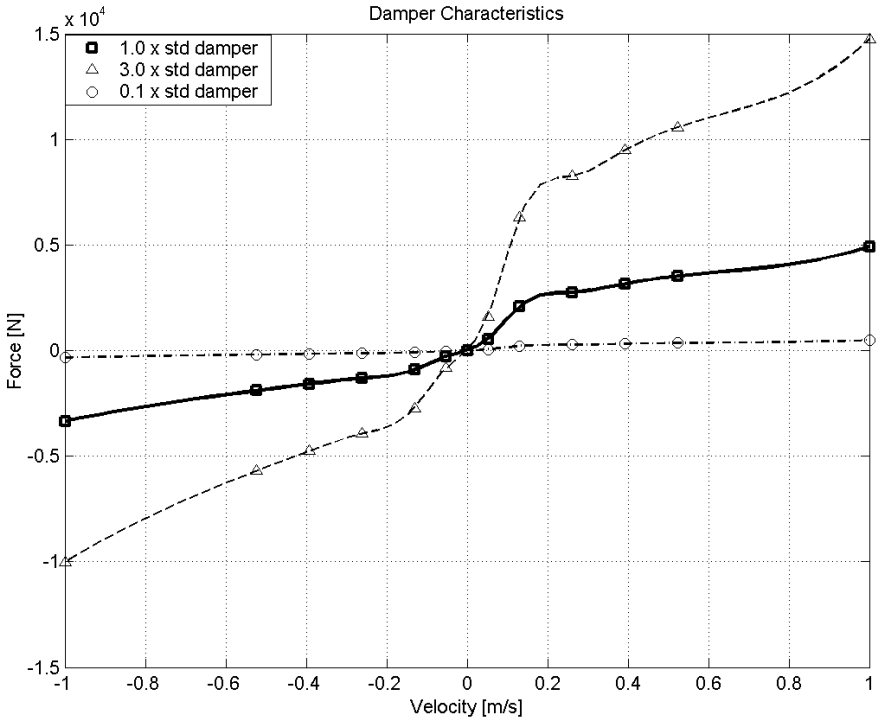

Figure 3.12: Definition of damper characteristics for various damper scale factors

where they may differ for front and rear (four design variables). The study is then extended to include seven design variables where the characteristics are identical front and rear, but the damper characteristics are defined by six design variables.

3.6.1 Two Variable Case

The two design variable study is an important starting point in the optimisation procedure, as it gives the necessary insight into the problem. For this two design variable study, it was decided to use the same design variables as those considered by Els and Uys [24] in their preliminary study, namely the static gas volume and the damper force scale factor. Figure 3.11 illustrates the spring characteristics for various static gas volumes. Figure 3.12 illustrates the damper characteristics for various damper scale factors.

The static gas volume is denoted by $gvol$, and the damper force scale factor by $dpsf$. These variables are allowed to range from 0.1 to 3 in magnitude, which are accordingly chosen as upper and lower bounds. The design

variables are explicitly defined as follows :

$$x_1 = dpsf, \qquad x_2 = gvol \tag{3.3}$$

with bounds

$$0.1 \leq x_i \leq 3, \qquad i = 1, 2 \tag{3.4}$$

3.6.2 Four Variable Case

For the four design variable problem the front and rear settings are uncoupled. This means that there are separate front and rear damper scale factors and front and rear spring static gas volumes. This results in two design variables describing the front and two describing the rear, giving four design variables in total.

The front damper scale factor is denoted by $dpsff$, the front static gas volume by $gvolf$, the rear damper scale factor by $dpsfr$, and the rear static gas volume by $gvolr$. These variables are also allowed to range from 0.1 to 3 in magnitude. Thus the design variables are defined explicitly as follows:

$$\begin{aligned} x_1 &= dpsff, \qquad x_2 = gvolf, \\ x_3 &= dpsfr, \qquad x_4 = gvolr \end{aligned} \tag{3.5}$$

with bounds

$$0.1 \leq x_i \leq 3, \qquad i = 1, ..., 4 \tag{3.6}$$

3.6.3 Seven Variable Case

For the seven design variable case the front and rear suspension characteristics are again identical as for the previous case with two design variables, however, the definition of the damper characteristic curve is given in terms of six variables. Although not considered in this study, the next step would be 14 variables allowing for the front and rear suspension to be uncoupled. The damper variables are defined in Figure 3.13. The variables for the problem are as listed in Table 3.5.

These variables vary over a range from 0.1 to 5000 in magnitude, so the problem needs to be scaled. For the purposes of scaling the current damper

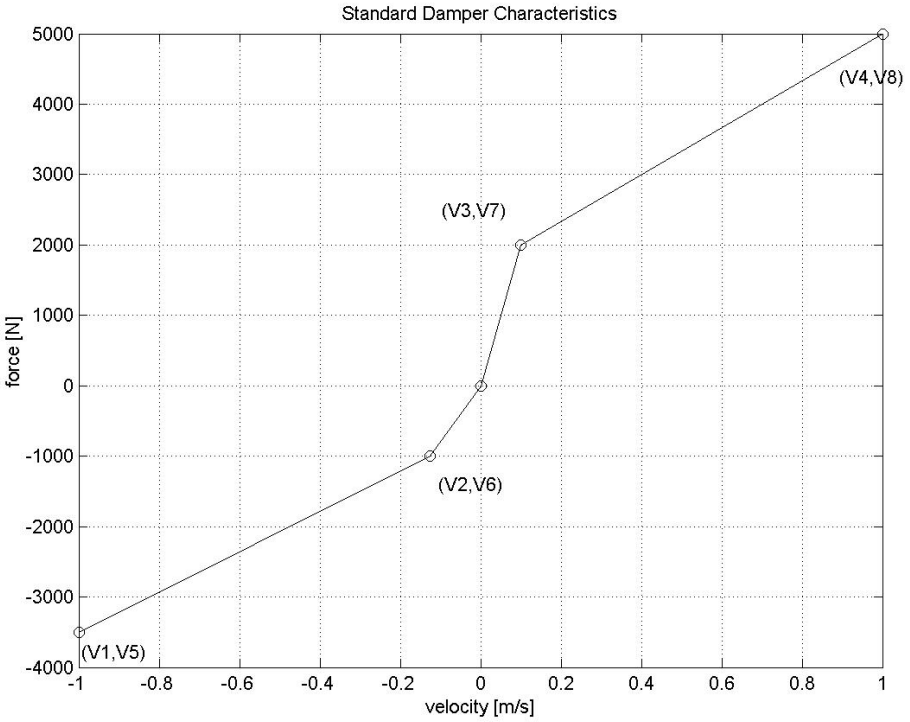

Figure 3.13: Definition of damper variables

Table 3.5: Definition of damper variables

gvol	Static Gas volume
V_1	High point negative velocity on damper graph
V_2	Change point negative velocity on damper graph
V_3	Change point positive velocity on damper graph
V_4	High point positive velocity on damper graph
V_5	Damper force corresponding to V_1
V_6	Damper force corresponding to V_2
V_7	Damper force corresponding to V_3
V_8	Damper force corresponding to V_4

setting values are used as scale factors. Variables V_1 and V_4 are kept at their original values so as to avoid convergence problems in the optimisation process. Problems were encountered when the value of V_4 was less than V_3 resulting in two possible forces for the same velocity. The ADAMS solver

cannot solve the dynamics of the system, as there exists two possible solutions for the same relative velocity between the vehicle body and axles. This leads to many discontinuities in the objective function. The design variables are thus defined as follows:

$$x_1 = gvol \tag{3.7}$$

$$x_2 = -\frac{V_2}{0.125} \qquad x_3 = \frac{V_3}{0.1} \tag{3.8}$$

$$x_4 = -\frac{V_5}{3500} \qquad x_5 = -\frac{V_6}{1000} \tag{3.9}$$

$$x_6 = \frac{V_7}{2000} \qquad x_7 = \frac{V_8}{5000} \tag{3.10}$$

with bounds

$$0.1 \leq x_i \leq 3, \qquad i = 1, ..., 7 \tag{3.11}$$

where

$$V_1 = -1, \qquad V_4 = 1 \tag{3.12}$$

According to the above scaling a design variable value of one for the damper settings will result in the current damper value. All the design variables have a range of 0.1 to 3, which defines the side constraints. For the purposes of this investigation it is assumed that V_8 can take on a value lower in magnitude than V_7. This is, however, very difficult to implement in practice, so for a passive damper, additional inequality constraints should be set. However, with the availability of the bypass valves on the semi-active unit, it is envisaged that this condition can be achieved.

3.7 Definition of Objective Functions

3.7.1 Ride Comfort

For ride comfort the motion of the vehicle is simulated for travelling in a straight line over the Belgian paving. The sum of driver and rear passengers

British Standard 6841 weighted root mean square (RMS) vertical accelerations [17], are used for the objective function. The motion sickness component was ignored as it requires long run times and the Belgian paving test track is not long enough to evaluate motion sickness. Both rear passenger and front driver RMS accelerations were considered for the ride comfort objective function, so as not to improve a single seat's comfort while severely decreasing the other seat's comfort.

3.7.2 Handling

For handling, the vehicle performs the ISO3888 [21] severe double lane change manœuvre at 80 km/h and the maximum body roll angle of the first peak [24], coinciding with the first steering input for the first lane change, is used as the objective function (Figure 3.14). This first peak is taken as the simulation is less likely to fail (vehicle roll over) due to the incorrect suspension setup, than looking at the last peak which is normally the most severe. This limits discontinuities in the design space. Roll angle is used as a measure of handling as suggested by Uys et al. [54] (Summarized in Appendix A), due to the linear relation observed between lateral acceleration and body roll angle. The minimization of vehicle body roll angle is a visual parameter that can easily be validated when the vehicles are tested.

The optimisation is performed with limited constraints, so as to allow for a better understanding of the performance requirements of the semi-active unit in attempting to achieve the optimisation objectives. The bounds on the design variables were the only constraints considered in this study.

3.8 Integration of Mathematical Vehicle Model and Optimisation Algorithms

In order to perform the optimisation process, it is desirable to have the optimisation algorithms and the mathematical simulation model working independently together, without user interaction. This is achieved by making use of the ADAMS Controls package which allows the user to define input

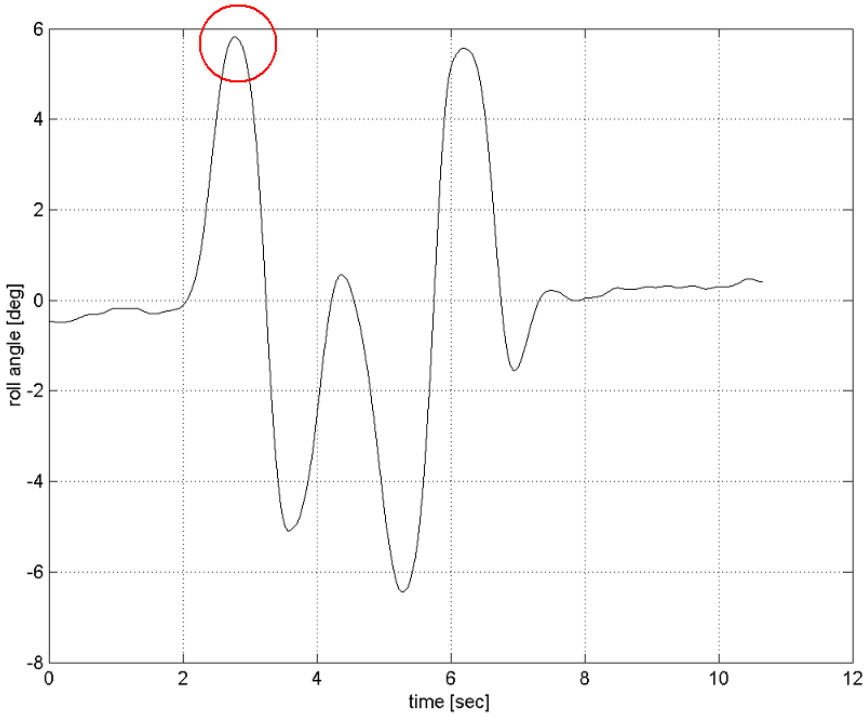

Figure 3.14: Body roll angle of a standard Land Rover Defender 110 while performing the double lane change manœuvre

and output data. This model can then be run from the Matlab Simulink environment. Figure 3.15 shows the vehicle model in Simulink with 9 input variables and the driver and passenger output results bins. The model can be run by the Matlab based optimisation codes by using the *sim* function. This model is then used for optimisation with respect to seven design variables.

3.9 Preliminary Sensitivity Investigations

3.9.1 Design Space

For the two design variable optimisation, surface plots of the objective function over the complete design space were generated. However, with an increasing number of variables added, this is not possible. These objective function surfaces were generated when the optimisation of handling (Figure 3.16) and ride comfort (Figure 3.17) were performed separately. From the figures it can be seen that for excellent handling capability, high damping

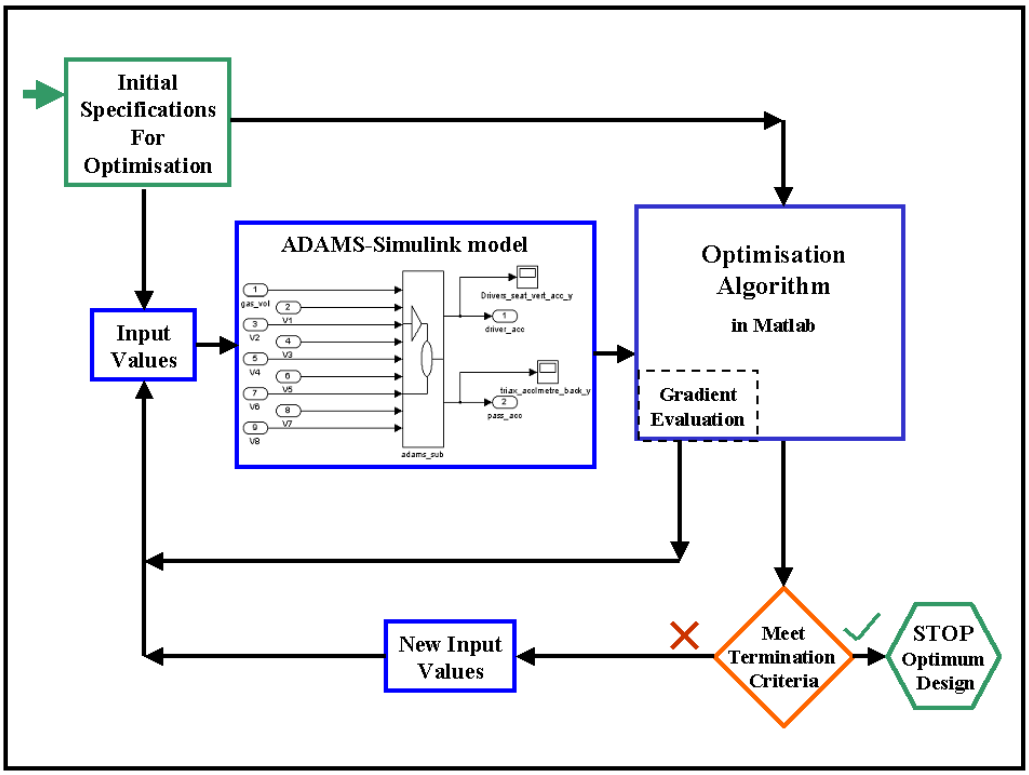

Figure 3.15: Optimisation process flow diagram

and high spring stiffness is required. The damping does not, however, contribute greatly to the improvement if the spring stiffness is high (a small gas volume)(Figure 3.16).

For ride comfort (Figure 3.17) on the other hand the opposite holds. Medium spring stiffness and low damping is required. The damper scale factor has a more noticeable effect on the ride comfort, as established previously by Els and Uys for the heavier version of this vehicle [24].

3.9.2 Gradient Sensitivity

Due to the complexity of the problem to be optimised, a few preliminary sensitivity investigations were required. The algorithms used in this study require gradient information for the optimisation process. This gradient information must be calculated using finite differencing methods. Gradient sensitivity studies were carried out in order to determine suitable values for the perturbations (dx_i) to be used for forward and central finite difference

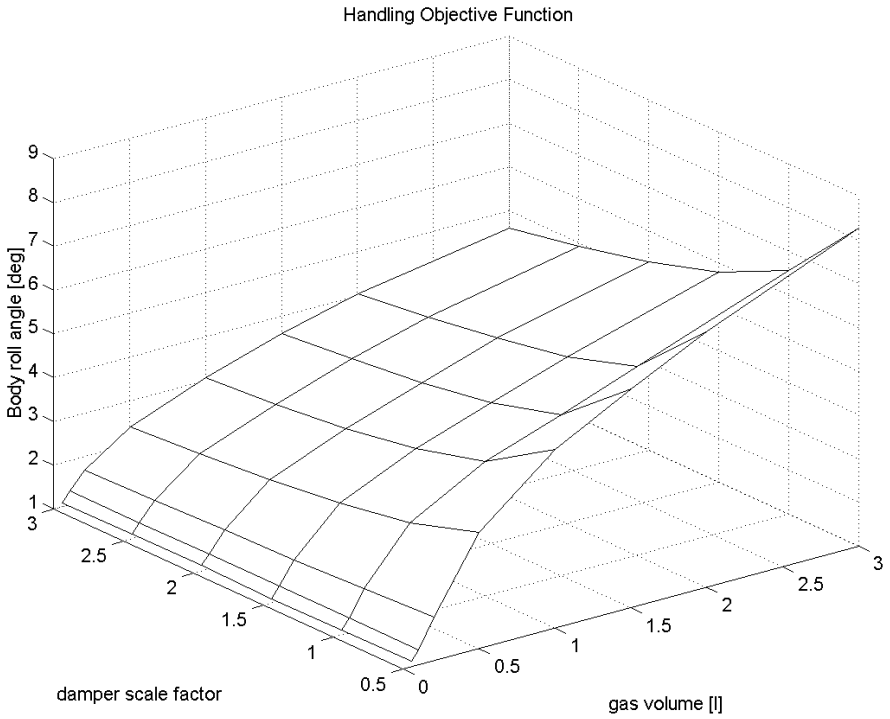

Figure 3.16: Vehicle roll angle, double lane change at 80 km/h for the two variable design space

gradients. The effects of the size of dx_i, for each variable, on the different gradient components, were evaluated and appropriate dx_i determined. From the gradient sensitivity studies it was observed that perturbations dx_i of around 0.1 were most appropriate for the optimisation problem.

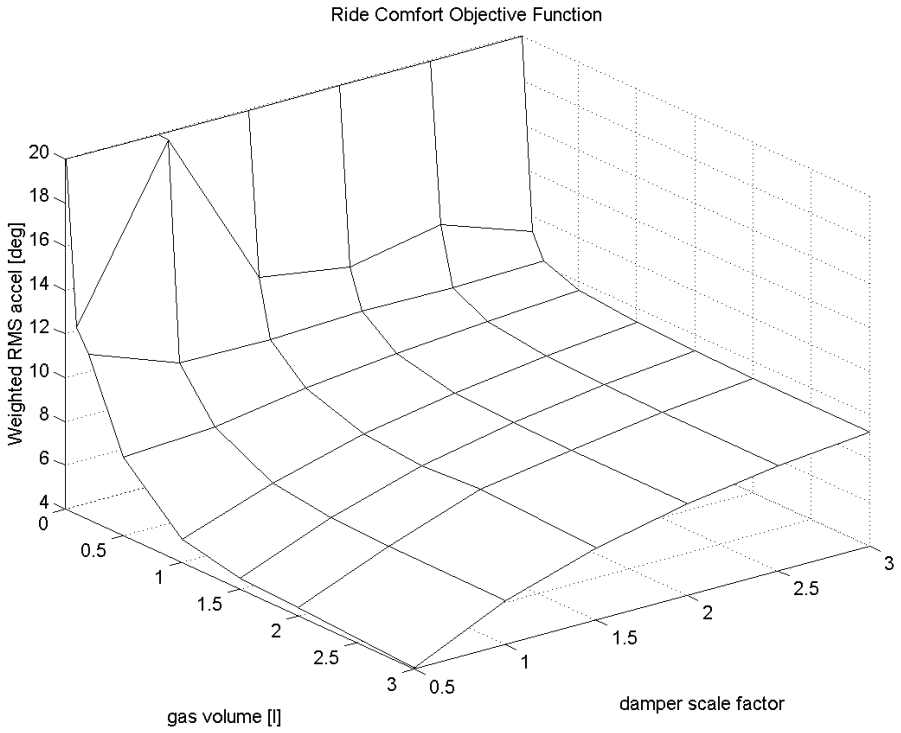

Figure 3.17: Vehicle ride comfort, Belgian paving at 60 km/h for the two variable design space

4. RESULTS

4.1 Handling Results

4.1.1 Two Design Variables

No serious problems were encountered in applying the algorithms to the optimisation of handling. For handling optimisation with two design variables no substantial difference can be reported between SQP and Dynamic-Q. The SQP convergence history for handling optimisation (Figure 4.1) indicates two local minimum solution sets with the same objective function value. The use of Dynamic-Q with 10 percent move limit (Figure 4.1) re-iterates the fact that design variable one (damper multiplication factor) has a limited effect on the handling objective function value as has already been established in Figure 3.16. Using a 20 percent move limit (Figure 4.1) Dynamic-Q progresses faster to a minimum. Because of the excellent performance of the forward finite difference method the use of central finite differences at additional cost was not necessary. The optima found by the optimisation algorithms are detailed in Table 4.1.

Table 4.1: Two design variable handling optimisation results

algorithm	func evals	$f(\mathbf{x}^*)$	x_1^*	x_2^*
DynQ 10 $^o/_o$	9	0.78	1.35	0.05
DynQ 20 $^o/_o$	9	0.81	1.99	0.05
SQP	21	0.78	1.60	0.05

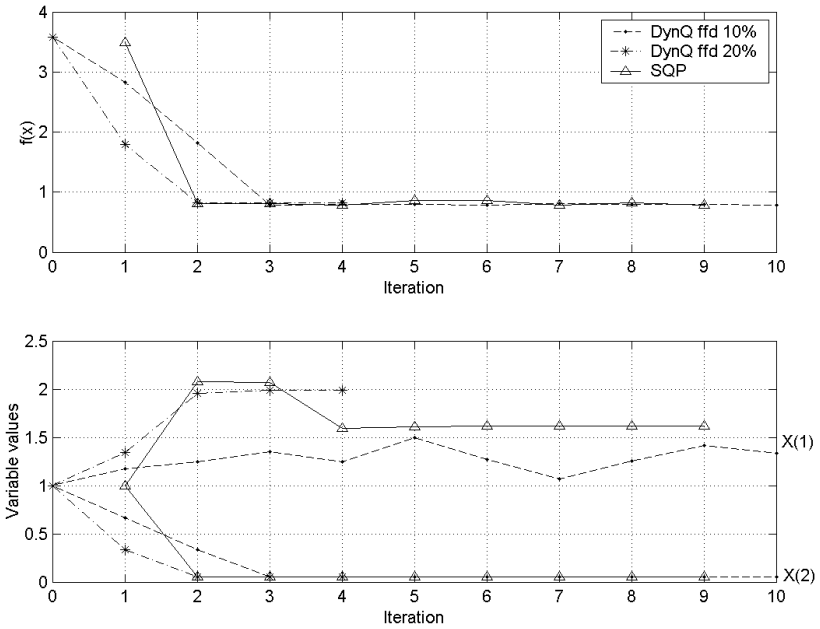

Figure 4.1: Optimisation histories of handling for two design variables

4.1.2 Four Design Variables

The handling optimisation results for four design variables (Figure 4.2) were not really different to that for two variables. This is as to be expected as the dynamics of the system has not changed substantially. It is interesting to note that a move limit of as big as 30 percent of the variables range may be used in Dynamic-Q using forward finite differences. It can also be seen from Figure 4.2 that the optimisation histories are very well behaved. Figure 4.2 again indicates the definite existence of more than one local minimum with the same objective function value. The SQP algorithm performed similarly to Dynamic-Q, and also found two different local minima, with the same objective function value. SQP converged in 9 iterations (49 function evaluations), compared to Dynamic-Q's 5 iterations (25 function evaluations). Table 4.2 compares the optimum values obtained using Dynamic-Q (with different move limits) to SQP. It can be seen that the gas volumes (x_2 and x_4) all ran to their respective lower bounds, while for the best roll angle, the damper scale factors (x_1 and x_3) went to their upper bounds, as happened in the case of the two design variable optimisation. The two different optima

correspond to the cases where the damper scale factors are respectively the same and different at the front and rear. The results here reinforce the initial conclusion from the results for two variables: that the damper scale factor has a negligible effect on the vehicle's handling performance (body roll angle) through the double lane change manœuvre at the optimum (stiff) spring rate. Although an improvement for the four design variable optimisation over the two design variable optimisation is expected, it was not realised as the lower limit set for the gas volume, in the two design variable case, is not physically feasible.

Table 4.2: Four design variable handling optimisation results

algorithm	func evals	$f(\mathbf{x}^*)$	x_1^*	x_2^*	x_3^*	x_4^*
DynQ 10 $^o/_o$	20	0.96	1.79	0.1	1.47	0.1
DynQ 20 $^o/_o$	25	0.95	3	0.1	2.90	0.1
DynQ 30 $^o/_o$	15	0.95	3	0.1	3	0.1
DynQ 45 $^o/_o$	15	0.95	3	0.1	2.97	0.1
SQP	17	0.96	1.49	0.1	1.44	0.1

4.1.3 Seven Design Variables

For the handling optimisation 9 design variables were initially used but it was found that this allowed too much freedom in the damper characteristics, resulting in two different forces for the same velocity. It was decided that the end velocities should be kept constant and only the interior velocity points moved by the optimisation algorithm, as defined in Section 3.6.3. Again the algorithms progressed quickly towards a local optimum. The best local optimum design states found by the algorithms are presented in Table 4.3. It is observed that the gas volume must be at the lower limit resulting in a very stiff spring characteristic. It can be observed that variables two and three must be at the lower bound, while variable five must be at the higher bound. The other damper variables do not appear to affect the performance of the vehicle substantially. A move limit in Dynamic Q up to 30

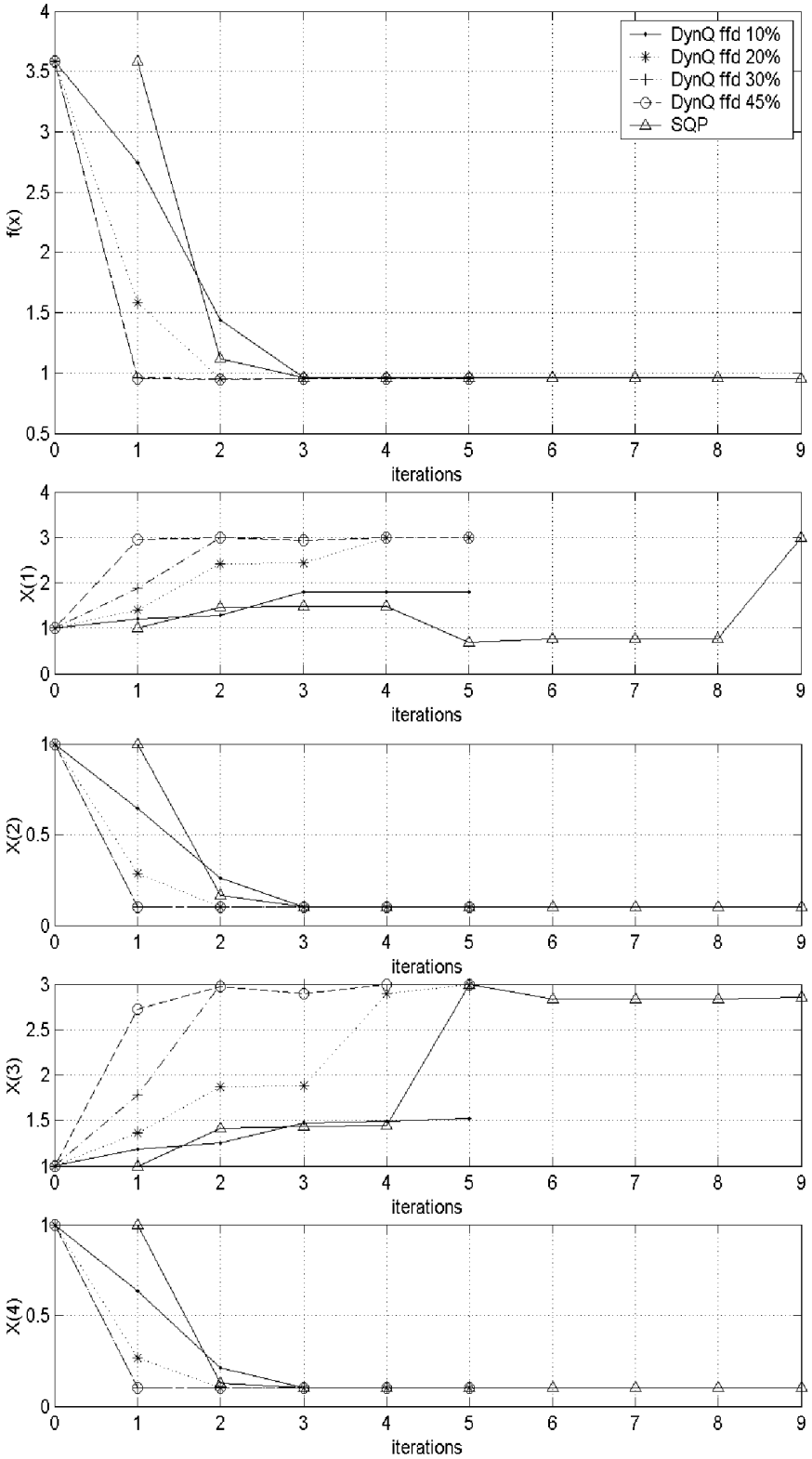

Figure 4.2: Optimisation histories of handling for four design variables

percent was found to arrive at the same optimum objective function value, with slight differences in the corresponding optimum design variables. The move limit was kept at 30 percent and a random starting point (Figure 4.3) tried with the same optimum area being reached. Figure 4.4 depicts the different optimum damper characteristics for handling obtained by the different optimisation algorithms. It is interesting to note that significantly different damper characteristics result in similar optimum behaviour. In the study by Naude [14] significantly different damper characteristics were found to result in similar optimum behaviour for the ride comfort optimisation. From Table 4.3 it can be seen that the SQP optimum found is significantly higher than that for Dynamic-Q, the results of this can be clearly seen by the completely different damper characteristic obtained in Figure 4.4. The SQP damper characteristic exhibits almost no damping force in the low speed region. It is generally accepted that high damping is required in the low speed region of the damper characteristic, for good handling. The optimum values are also lower than for the four design variables, but it must be remembered that for the seven design variables the front and rear suspension characteristics are the same, unlike for four design variables where the front and rear suspension characteristics may differ.

Table 4.3: Seven design variable handling optimisation results

algorithm	func evals	$f(\mathbf{x}^*)$	x_1^*	x_2^*	x_3^*	x_4^*	x_5^*	x_6^*	x_7^*
DynQ ffd 10 $^o/_o$	48	1.04	0.1	0.1	0.1	0.63	3	1.40	1.45
DynQ ffd 20 $^o/_o$	40	1.02	0.1	0.1	0.1	2.07	3	1.83	1.24
DynQ ffd 30 $^o/_o$	64	1.05	0.1	0.1	0.96	2.68	3	3	2.06
DynQ rand 30 $^o/_o$	48	1.05	0.1	0.1	0.1	0.1	3	0.90	0.1
SQP	52	1.34	0.1	1.78	1.38	1.85	3	0.1	2.21

Figure 4.5 takes all the points obtained in the optimisation history and evaluates the Euclidean-norm distance of the points from the found minimum. This distance is then plotted against its corresponding objective func-

tion value. This gives a general indication of the robustness of the minimum point. From this it can be seen that for all the minima found by the algorithms, the objective function value does not change significantly when a move limit of 1.5 from the optimum, subject to design variable x_1 (gas volume) being at its lower bound. Above 1.5 the Dynamic-Q with 10 percent move limit becomes difficult to predict. However, there exists many local minima at a Euclidean-norm distance of more than 2 away from the current optimum points. This is, however, not a complete picture of the situation, as not all the variables can change as much as others due to the insensitivity of some variables, such as x_6 and x_7, on the objective function.

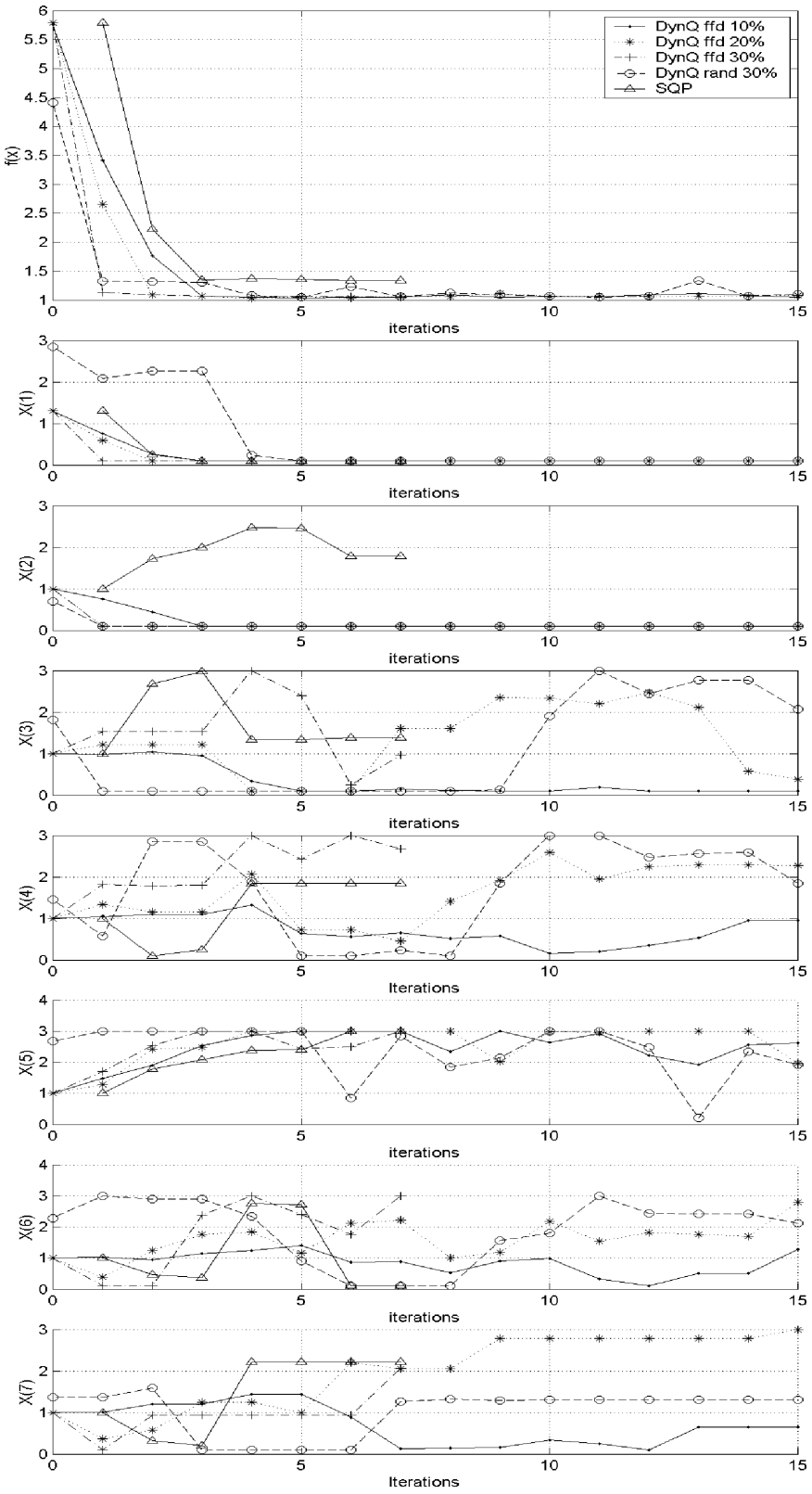

Figure 4.3: Optimisation histories of handling for seven design variables

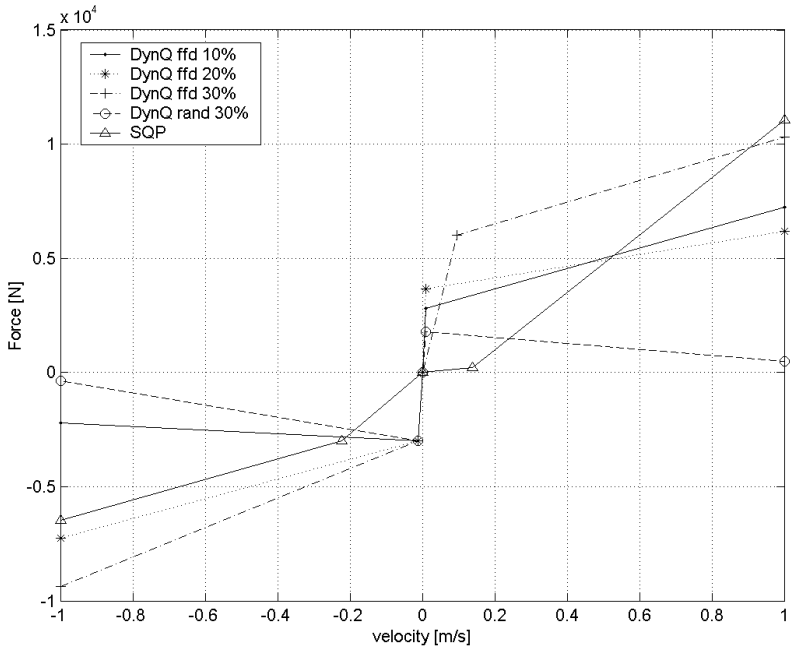

Figure 4.4: Optimum damper characteristics for handling

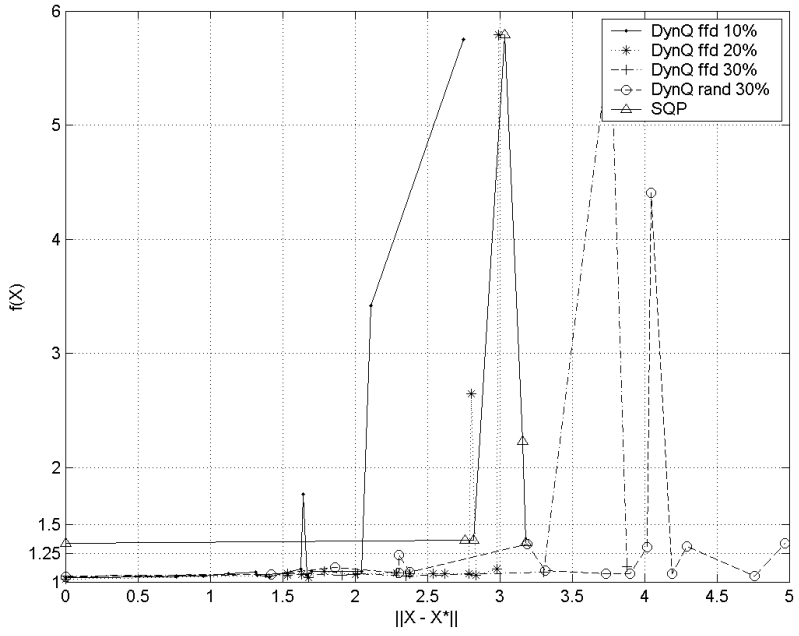

Figure 4.5: Existence of many local minima away from current optimum, for the seven design variable, handling optimisation

4.2 Ride Comfort Results

4.2.1 Two Design Variables

The two design variable ride comfort optimisation encountered problems associated with a noisy objective function. The SQP method (Figure 4.6) took eight iterations (33 function evaluations) to stabilize at the minimum, which corresponds to the lowest possible damping and stiffness values, as expected from Figure 3.17, and also corresponds to the prescribed lower bounds of the variables. The Dynamic-Q method, on the other hand, experienced greater difficulty in reaching a stable minimum. The central finite difference method was introduced to evaluate the gradient of the objective function in an attempt to obtain stability in the optimisation process. The Dynamic-Q method with central finite differences, with a ten percent move limit (Figure 4.6) took nine iterations (50 function evaluations) to find a minimum. Inspection of the results shows that this minimum is effectively reached after only four iterations (25 function evaluations). The vertical acceleration at this point is, however, significantly higher than that found with SQP, indicating the existence of a separate interior local minimum. A 20 percent move limit (Figure 4.6) took six iterations (30 function evaluations), finding a local minimum not far off the SQP minimum, but still lying within the bounds of the feasible region. It should be noted that the Dynamic-Q minimum design variable values found in this case are not at the extrema found by the SQP method. This reinforces the fact that the ride comfort design space has a flat plateau with multiple local minima.

Table 4.4: Two design variable ride comfort optimisation results

algorithm	func evals	$f(\mathbf{x}^*)$	x_1^*	x_2^*
DynQ cfd 10 $^o/_o$	25	4.14	0.37	1.44
DynQ cfd 10 $^o/_o$	50	4.07	0.39	1.60
DynQ cfd 20 $^o/_o$	30	3.22	0.25	2.50
SQP	33	2.70	0.11	3

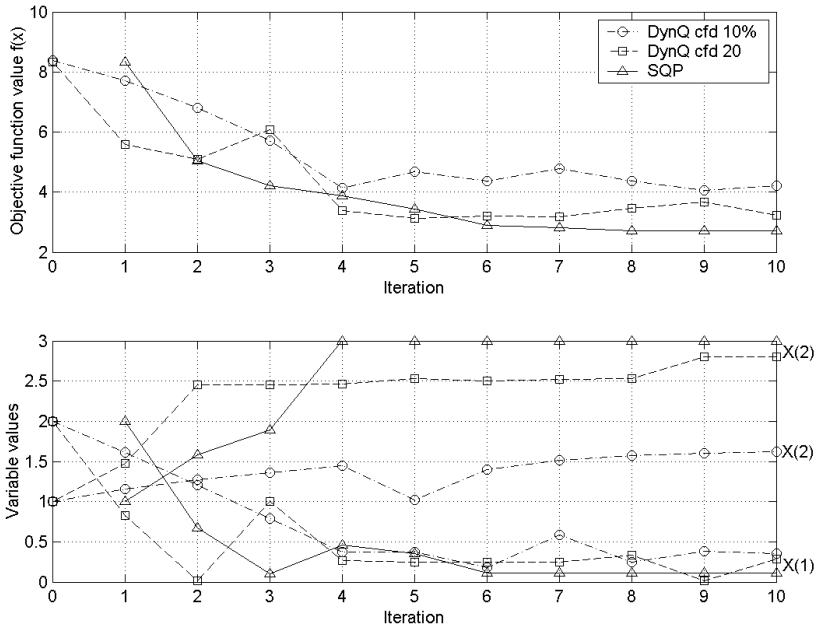

Figure 4.6: Optimisation histories of ride comfort for two design variables

4.2.2 Four Design Variables

For the four design variable optimisation, Dynamic-Q was modified so that the move limit for each iteration is 90 percent of the move limit of the previous iteration. This was done to stabilize the convergence behaviour of the algorithm, and to try and prevent high spikes in the optimisation process. These spikes are caused by a poor approximation to the objective function close to the minimum. This results in the LFOPC algorithm finding a minimum of the approximate problem, on the slope of the steep valley, very close to the actual minimum. Indicative of the close proximity to the minimum is the fact that, in spite of the large spike at iteration six, the corresponding changes in the variables are very small. However, Dynamic-Q quickly recovers within a single iteration (5 function evaluations) as can be seen at iteration seven in Figure 4.7. When looking at the Euclidean-norm distance from the optimum, it is observed that although the objective function experiences an increase in value at iteration 6, the Euclidean-norm distance from the optimum is decreasing, proving that Dynamic-Q is converging towards the optimum.

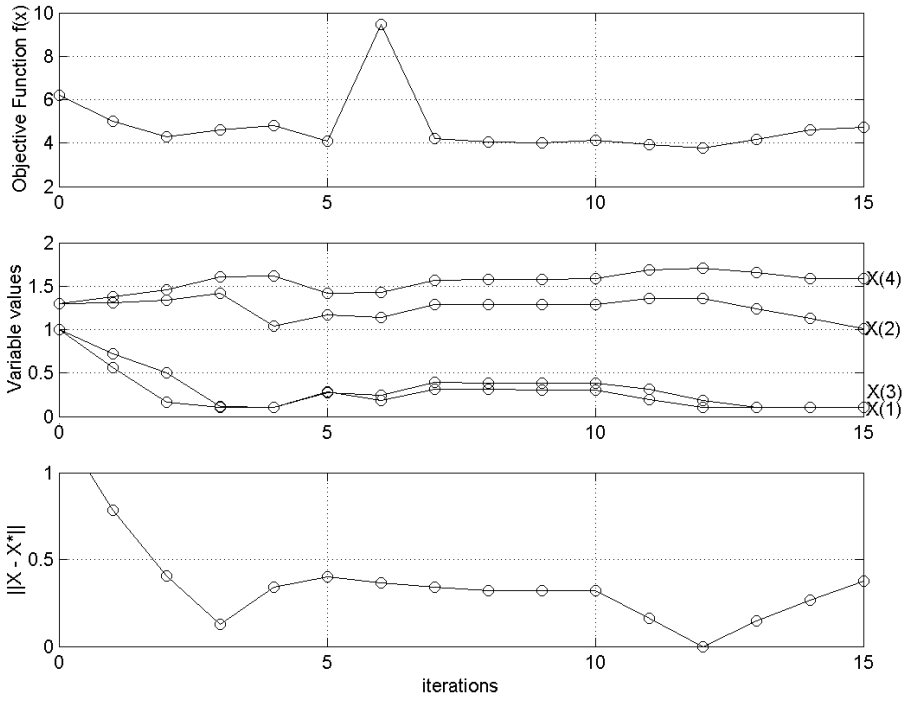

Figure 4.7: Dynamic-Q ffd ride comfort, 4 design variables, 10 percent move limit, gas volume range from 0.1 to 3 litres

The results of the optimisation are presented in Figure 4.8 for both central finite differences and forward finite differences used for the gradient approximations. From Figures 4.7 and 4.8 for the forward finite difference Dynamic-Q implementation, it can be seen that the smaller move limit of 5 percent is more stable, reaching a minimum within 6 iterations (35 function evaluations), while a 10 percent move limit takes 12 iterations (65 function evaluations). The algorithm, however, does not converge due to the noisy objective function with steep valley. The convergence behaviour for central finite differences coupled to Dynamic-Q is shown in Figure 4.8 requiring four iterations (45 function evaluations). Again it has been determined that the smaller move limit improves convergence to the minimum. The central finite difference gradient evaluation builds into the system a level of robustness. From the results in Table 4.5 it can be seen that a value of around 1.5 litre gas volume (x_2 and x_4), and limited damping (x_1 and x_3), returns the best results. From the central finite difference results, it can be seen that an in-

creased rear gas volume x_4, with minimal damping x_3, compared to the front, results in a better overall ride comfort (Figure 4.8).

Table 4.5: Effect of changing the gas volume range for four variable ride comfort optimisation

algorithm	Func evals	$f(\mathbf{x}^*)$	x_1^*	x_2^*	x_3^*	x_4^*
$0.1 \leq gvol \leq 3$						
DynQ ffd 10 $^o/_o$	65	3.77	0.18	1.36	0.10	1.70
DynQ ffd 5 $^o/_o$	35	3.85	0.48	1.44	0.14	1.60
DynQ cfd 10 $^o/_o$	45	3.61	0.31	1.32	0.24	2.04
SQP	65	3.49	0.19	2.08	0.35	2.18
$0.008 \leq gvol \leq 0.5$						
DynQ cfd 10 $^o/_o$	108	7.24	0.60	2.98	0.72	3
DynQ cfd 5 $^o/_o$	144	7.40	0.53	2.68	0.74	3
DynQ ffd 10 $^o/_o$	65	7.19	0.90	3	0.16	3
DynQ ffd 5 $^o/_o$	80	8.71	0.64	1.28	0.56	2.37
SQP	114	9.32	0.14	0.94	0.99	1.90
infeasible starting point for $0.008 \leq gvol \leq 0.5$						
DynQ ffd 10 $^o/_o$	65	8.10	2.62	1.76	0.30	3
SQP	94	7.80	2.96	2.08	0.08	3
$1.03 \leq gvol \leq 3.0$						
DynQ cfd 10 $^o/_o$	99	2.86	0.33	1.81	0.05	3
DynQ cfd 5 $^o/_o$	117	3.39	0.33	1.15	0.19	1.36
DynQ ffd 10 $^o/_o$	70	3.46	0.24	1.06	0.15	1.61
DynQ ffd 5 $^o/_o$	50	3.49	0.36	0.89	0.25	1.48
SQP	111	3.59	0.29	1.06	0.28	1.10
started at predicted minimum from 2 variable optimisation						
DynQ cfd 10	126	2.67	0.19	2.83	0.05	2.96

SQP also found similar improved results within 8 iterations (65 function evaluations) (Figure 4.8). From Table 4.5 it is concluded that Dynamic-Q, with forward finite differences, does not reach the same minimum as

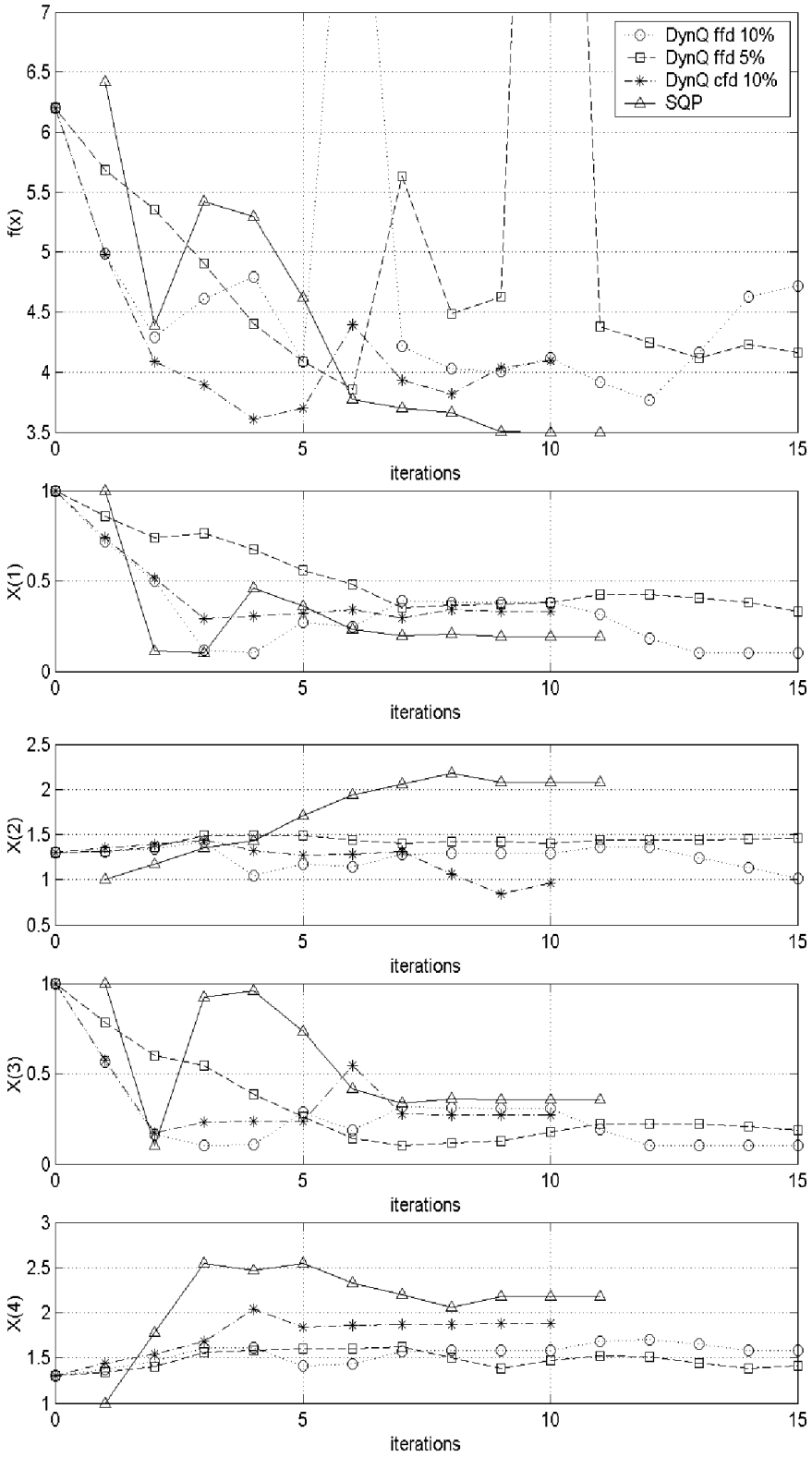

Figure 4.8: Optimisation histories of ride comfort for four design variables (gas volume range from 0.1 to 3 litres)

Dynamic-Q with central finite differences. The performance of Dynamic-Q with central finite differences is also relatively economic, compared to that of SQP, finding a minimum within five percent of the SQP minimum objective function value. Again it was found that SQP has a tendency to run to the boundaries. The reason for this is because the optimum of the approximated sub-problem may lie outside the boundary. SQP then sets the violating variables to their boundary values and finds the optimum from the boundary by performing line searches. Quite often it finds that the previous minimum is not at the boundary for a specific variable, but because the gradient indicates that going in the direction of the boundary decreases the function value, it returns to the boundary point for the next iteration. If found that this new point has a higher function value than the previous function value, SQP performs a few line searches until a minimum lower than previously is found. SQP thus gets stuck in a region which is not the case with Dynamic Q, where the move is more rigorously controlled by the move limit setting. Dynamic-Q will thus move more gradually to the optimum, while SQP jumps faster to a minimum, at the boundary, and such a jump may, as in this case, fortuitously give the lowest function value.

The SQP minimization is better understood with reference to Figure 4.9 giving a schematic representation of the optimisation, with respect to one variable. Consider starting point a. At this point the objective function is approximated using a quadratic approximation. The optimum of this function is at a*, resulting in b being the next iteration point. The approximate optimum b* now lies outside the feasible region, thus the variable is set to the boundary value, resulting in iteration point c with minimum point c*. In turn c* gives d as a minimum, and thus the approximation leads back to the boundary at point d*. The next iteration point would be e1, however, here the objective function value is significantly higher than that for the previous iteration value d. A line search is done to obtain point e in the region of iteration d, resulting in another boundary approximated iteration point. The SQP algorithm thus gets stuck in the region of d and e.

Because of the boundary clinging nature of SQP, and Dynamic-Q's dif-

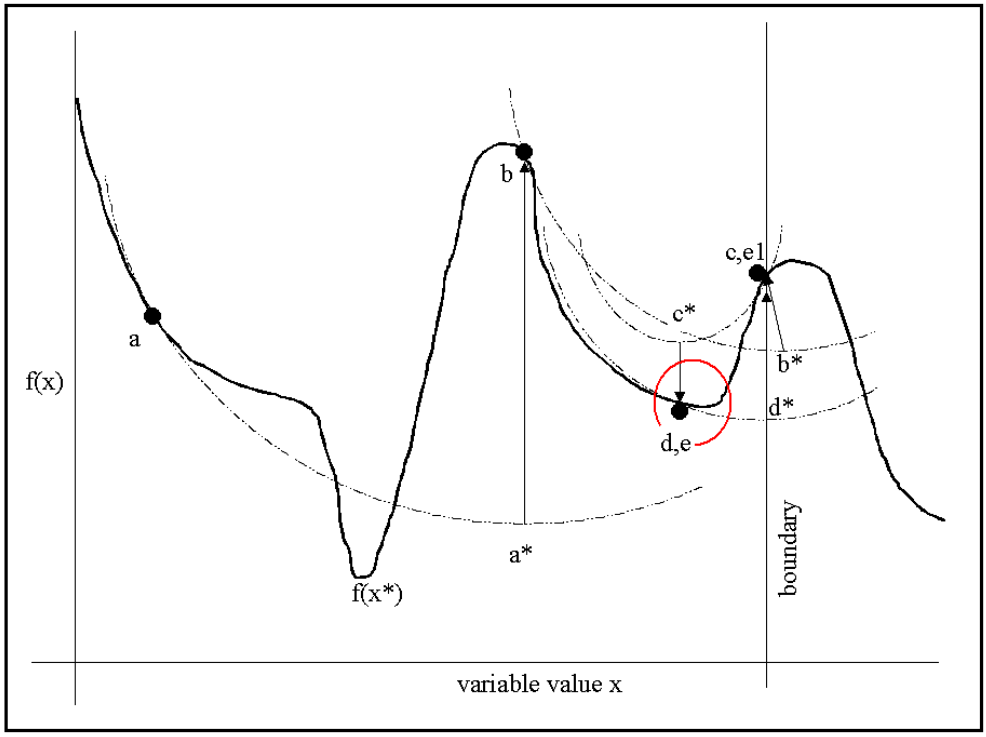

Figure 4.9: SQP optimisation movements

ficulty in handling this noisy objective function space, the design space for the gas volumes was split. This was done by imposing the 0.05 to 3 side constraints on the variables and by changing the definition of the gas volume variables as follows:

$$gvolf = \frac{1}{6}x_2 \tag{4.1}$$

for the front, and

$$gvolr = \frac{1}{6}x_4 \tag{4.2}$$

for the rear. The gas volume now has a range between 0.008 and 0.5 litres, which is practically more realizable than the initial upper boundary of 3 litres. From Figure 4.10 it is observed that there is little difference in the convergence behaviour of Dynamic-Q with central finite differencing and forward finite differencing. It is also observed, that the convergence histories are much smoother, not exhibiting the spikes previously observed. The main reason for this, is attributed to the fact that the gas volume variable is not permitted

to reach into the flat plateau region. The optimum objective function values (Table 4.5) are significantly higher than previously obtained, indica-ting that the gas volume range is too limiting. Optimisation runs were performed from the infeasible region, with the SQP method finding a better optimum than when started in the feasible region. Dynamic-Q, however, needed more iterations than the limited 15 iterations that it was permitted to perform. This is probably because the SQP method sets all initial starting design values, outside the feasible region, to their boundary values, while Dynamic-Q gradually progresses from its given starting design variable values. Although some of the starting points were outside the boundaries, none of the boundaries were violated for the optimum design conditions obtained. However, almost all algorithms found optima where the rear gas volume design variable x_4, was lying on the upper boundary, resulting in a gas volume of 0.5 litres.

Because of the improved behaviour obtained, the gas volume was modified again to look only at the flat plateau region of the design space. The design variables relating to the gas volume are defined as follows:

$$gvolf = \frac{2}{3}x_2 + 1 \tag{4.3}$$

for the front, and

$$gvolr = \frac{2}{3}x_4 + 1 \tag{4.4}$$

for the rear. This means that the gas volume can range between 1 and 3 litres for a variable range of 0.05 to 3. As was to be expected (Figure 4.11) many problems were experienced with convergence, due to the noisy nature of the objective function. Table 4.5 summarizes the results for the different gas volume ranges. Again, none of the boundary constraints were violated. It can be seen that Dynamic-Q with central finite differences and a 10 percent move limit, obtained the most optimum objective function values, with the rear gas volume at its upper bound and damper scale factor at its lower bound. It is also interesting to note that even when started at the predicted minimum for the two design variable optimisation, the Dynamic-Q method with central finite differences took as many as 13 iterations (126 function evaluations) to obtain the minimum.

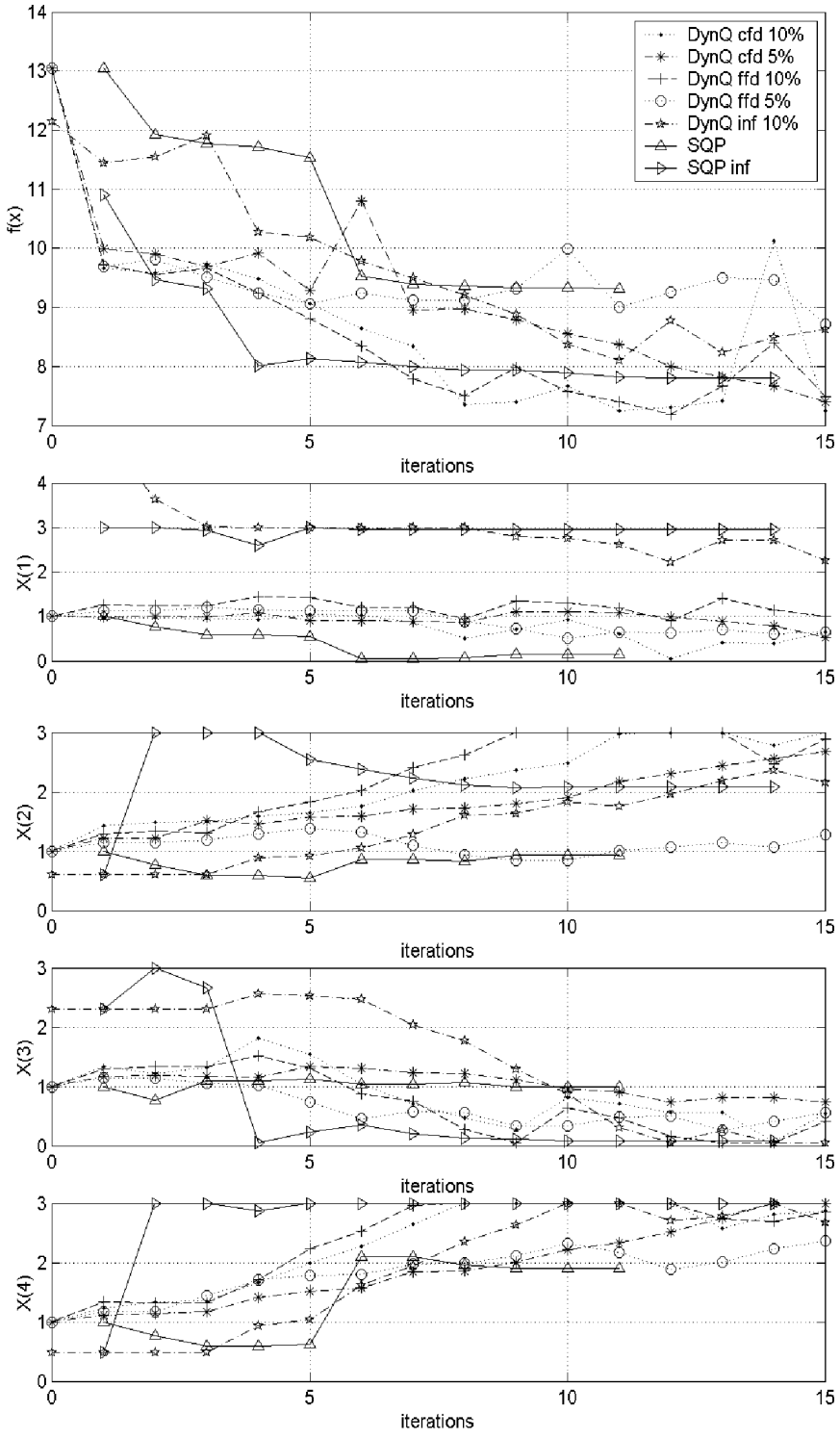

Figure 4.10: Optimisation histories of ride comfort for four design variables (gas volume ranges from 0.008 to 0.5 litres, with inf - being an infeasible starting point)

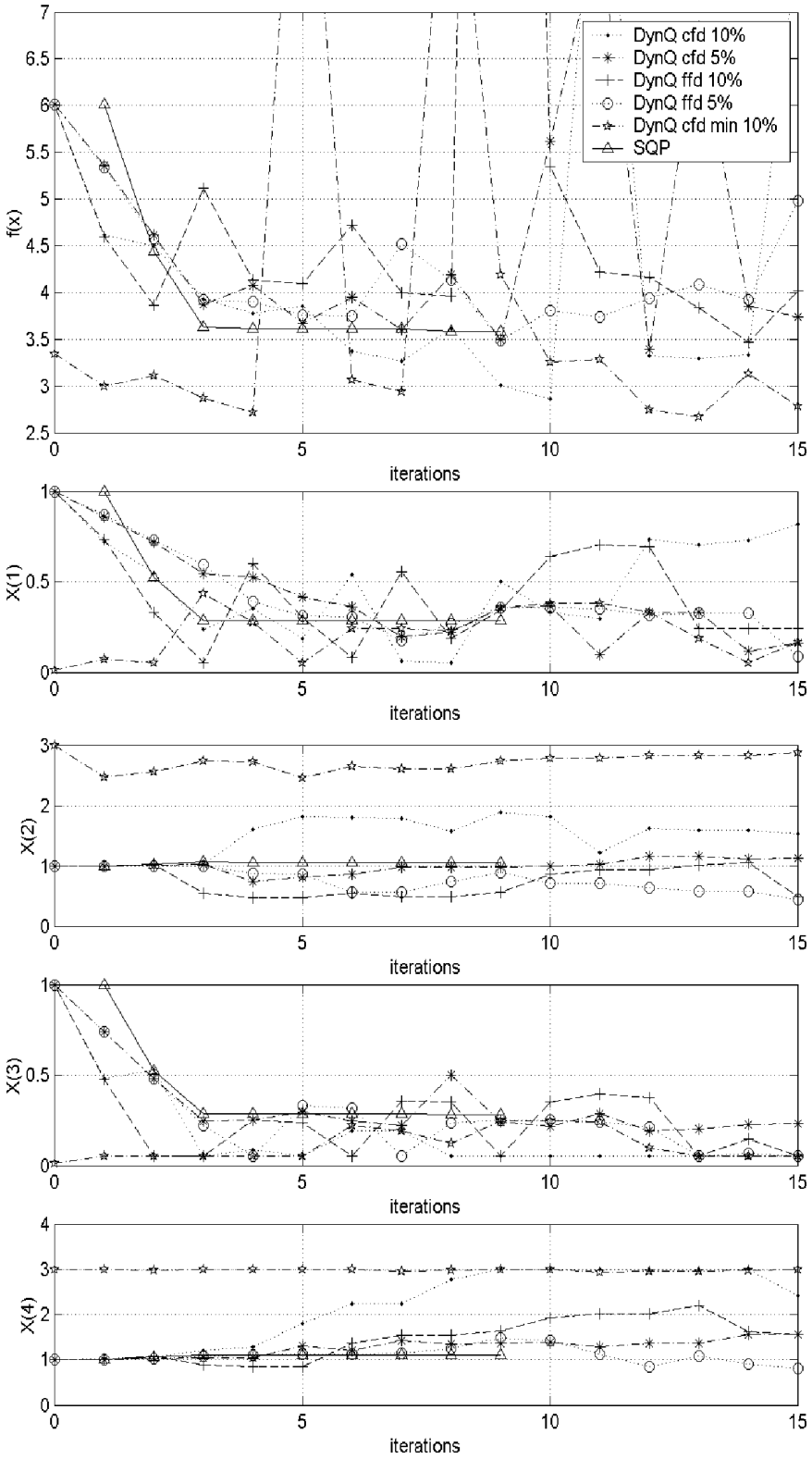

Figure 4.11: Optimisation histories of ride comfort for four design variables (gas volume range from 1.03 to 3 litres)

4.2.3 Seven Design Variables

Figure 4.12 illustrates the gradual convergence of Dynamic-Q towards the local minimum, while it can be clearly seen how SQP jumps and gets stuck in converging to a minimum. While gradual convergence can be seen as both advantageous and disadvantageous for the problem at hand, the gradual movement into and out of the local minimum is viewed as more favourable. It gives more insight into the robustness of the design corresponding to the local minimum, and also has a greater probability of finding a better minimum, that would otherwise have been the case. It is interesting to note that Dynamic-Q with central finite differences and a ten percent move limit, obtained the same optimum objective function value (Table 4.6) as Dynamic-Q with forward finite differences and a five percent move limit, but not corresponding to the same combination of variable values. This again reinforces the belief that the ride comfort objective function exhibits a region with various local minima. It is also of interest to note that a gas volume of 1.77 litres is found as an optimum value by using SQP. Although this value differs significantly from that found by Dynamic-Q, the objective function value is more or less the same. The damper characteristics are vastly different for the different local optima found (Figure 4.14). It is important to note that for negative damper velocities the ideal damper characteristics mostly take on a negative gradient, corresponding to a damping coefficient of -1250 Ns/m, or positive gradient corresponding to 830 Ns/m . Again, a number of design variables (x_2, x_3, x_4) assume their lower boundary values in the case of SQP.

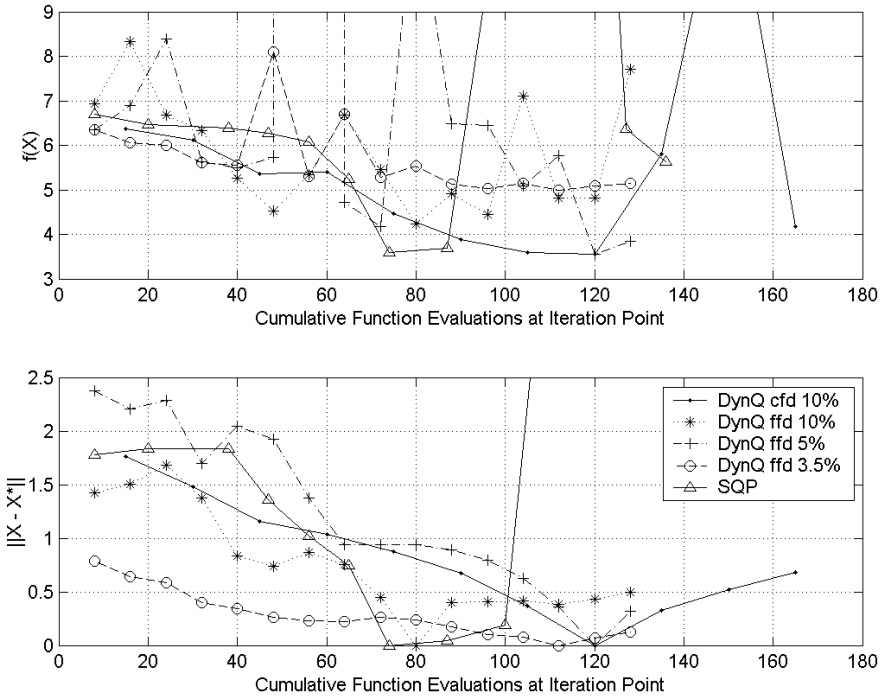

Figure 4.12: Convergence to optimum, seven design variables

Table 4.6: Seven variable ride comfort optimisation results

algorithm	Func evals	$f(\mathbf{x}^*)$	x_1^*	x_2^*	x_3^*	x_4^*	x_5^*	x_6^*	x_7^*
DynQ cfd 10 $^o/_o$	120	3.55	2.23	1.28	1.49	0.23	0.10	0.66	0.38
DynQ ffd 10 $^o/_o$	150	4.24	1.56	0.49	0.88	0.31	1.78	0.55	0.42
DynQ ffd 5 $^o/_o$	120	3.55	2.48	2.26	1.15	0.11	0.86	0.20	0.38
DynQ ffd 3.5 $^o/_o$	112	4.99	1.07	1.06	0.75	0.49	0.90	0.82	0.50
SQP	74	3.57	1.77	0.1	0.1	0.1	1.14	0.84	0.40

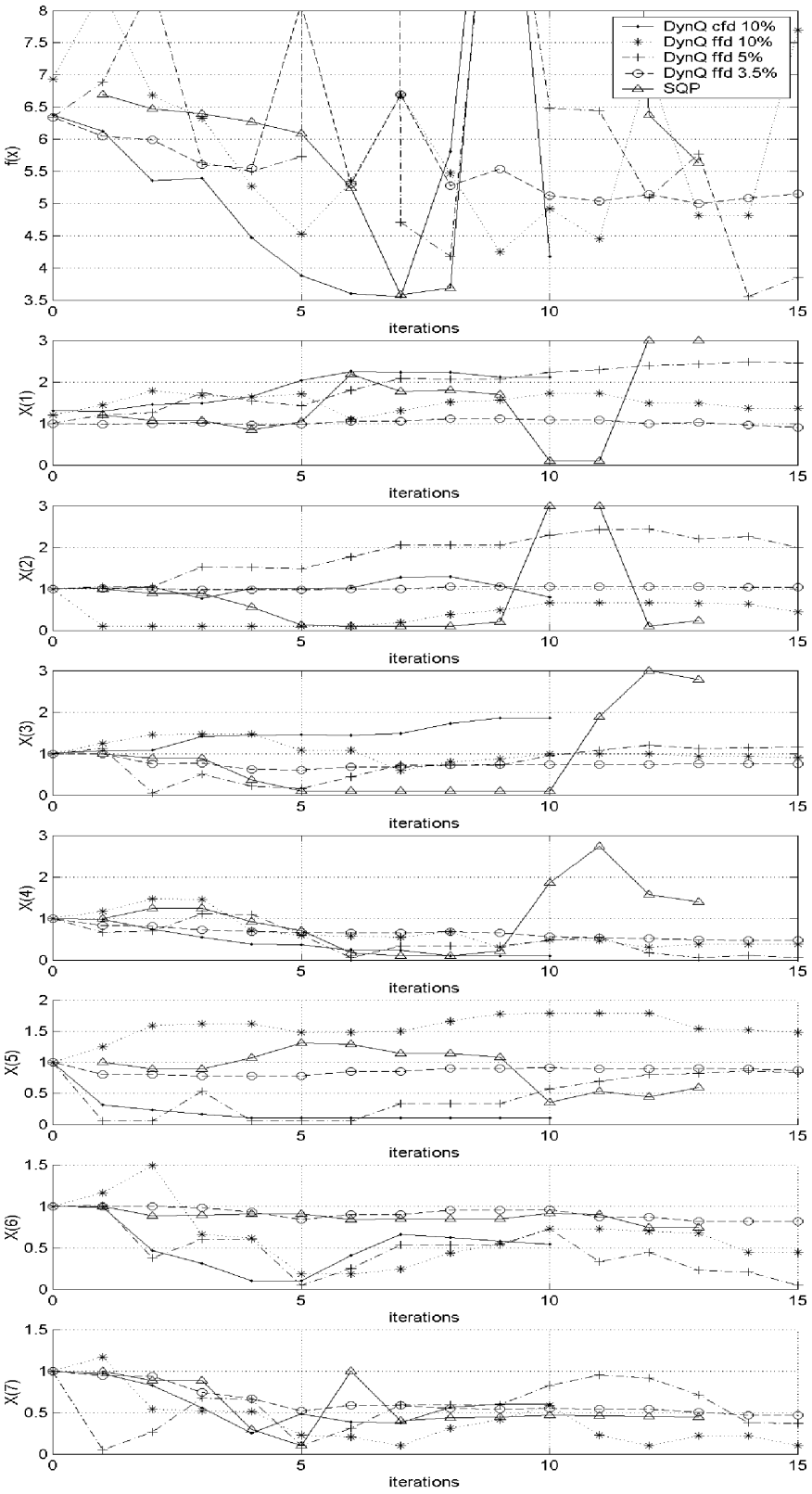

Figure 4.13: Optimisation histories of ride comfort for seven design variables

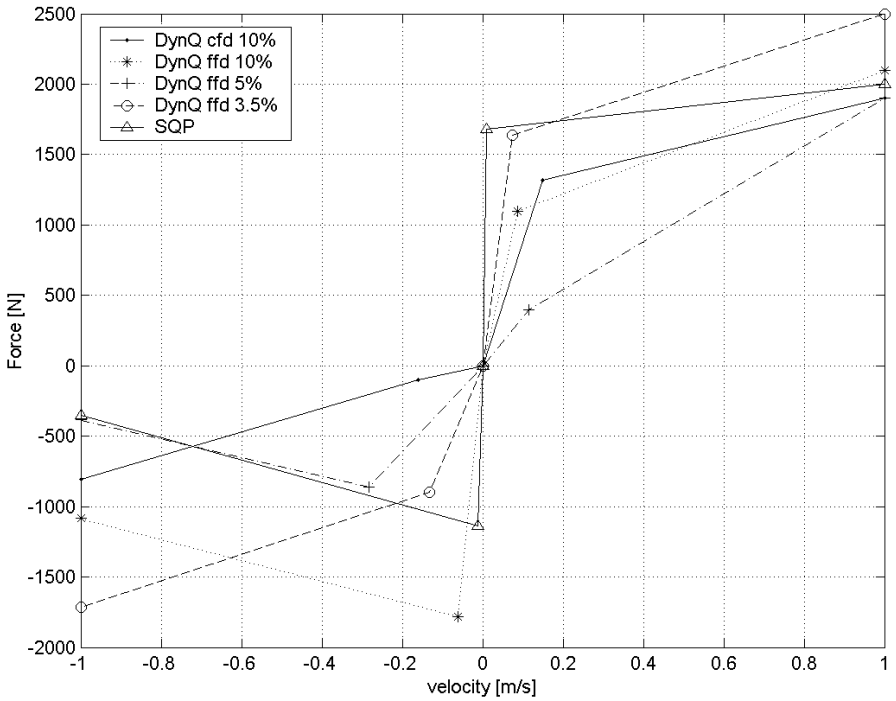

Figure 4.14: Optimum damper characteristics for ride comfort

5. DISCUSSION OF CONCLUSIONS

The integration of the optimisation algorithms with the full multidimensional vehicle model has been successfully achieved, allowing for an automated optimisation process. It has also been shown that fundamental gradient-based optimisation algorithms can be successfully applied to the optimisation of the vehicle's suspension system for both ride comfort and handling.

The use of central finite differences has been shown to offer substantial benefits, if noise is present in the objective and constraint functions, as is the case with the ride comfort optimisation. The central finite differences allows for better approximations to the gradients of the objective and constraint functions, and leads to more promising results, without too high a penalty being paid in terms of number of objective functions needed to obtain convergence.

Although for the ride comfort optimisation Dynamic-Q generally took more function evaluations than SQP, it found the local minima by moving within the whole design space. In most cases SQP jumped from boundary to boundary, finding the local minimum from the boundaries. SQP might therefore miss local minima that do not lie close to the design space boundaries. Thus it can be concluded that Dynamic-Q is a competitive and reliable alternative to SQP for vehicle suspension design.

6. DISCUSSION OF FUTURE WORK

Only a limited number of design variables have been considered here. It is believed that Dynamic-Q will come into its own when more variables are considered. The next step in the optimisation will be to change the front and rear spring and damper characteristics independently. This will result in fourteen design variables.

On the algorithmic side the study shows that, a better and desirable convergence behaviour is obtained for Dynamic-Q if smaller move limits are specified. It would be interesting to see how much of an improvement the use of central finite differences would give when used in SQP, as opposed to the forward finite differences used in this study.

A greater variety of road conditions need to be considered over varying vehicle speeds and loading conditions, before a decision can be made regarding the final overall optimum design. The ultimate test will be the optimisation of the vehicle's performance under severe handling manœuvres on a rough track. More efficient tyre models should ideally also be considered, in order to achieve better correlation with measured track results. The incorporation of the complex model describing the hydro-pneumatic suspensions characteristics as proposed by Theron [55], should be included in the next optimisation phase.

The final optimised spring and damper characteristics should be investigated for robustness. This should be done in terms of the effect normal manufacturing tolerances will have on the vehicle's handling and ride comfort.

BIBLIOGRAPHY

[1] The International Organisation for Standardisation: Mechanical Vibration - Road Surface Profiles - Reporting of Measured Data. *ISO 8608* (01 September 1995).

[2] Hall, L.C.: Terrain Profile Characteristics. *Fundamentals of Terramechanics and Soil Vehicle Interaction, Wheels and Tracks Symposium, Cranfield University* (9-11 September 1998)

[3] Bakker, E., Pacejka, H.B., Linder, L.: A New Tire Model with an Application in Vehicle Dynamics Studies. *SAE 890087.*

[4] Van Oosten, J.: Tyre Modelling Overview Adams(/Car) Tyre Modelling. *ADAMS Users Conference* November (2002).

[5] Using ADAMS Tyre Tyre Models. *Mechanical Dynamics* (2002).

[6] Van Oosten, J.J.M., Bakker, E.: Determination of Magic Tyre Model Parameters. 1^{st} *International Colloquium on Tyre Models for Vehicle Dynamics Analysis* October (1991).

[7] FTire Flexible Ring Tyre Model ADAMS Version - Documentation and User's Guide. *Cosin Consulting* (5 June 2002).

[8] Duym, S.W., Steins, R., Baron, G.V., Reybrouck, K.G.: Physical Modelling of the Hysteretic Behaviour of Automotive Shock Absorbers. *SAE 970101.*

[9] Duym, S., Stiens, R., Reybrouck, K.: Evaluation of Shock Absorber Models. *Vehicle System Dynamics* 27 (1997), pp. 109–127.

[10] Eberhard, P., Bestle, D., Piram, U.: Optimisation of Damping Characteristics in Nonlinear Dynamic Systems. *First World Congress of Structural and Multidisiciplinary Optimisation* (1995), pp. 863–870.

[11] Etman, L.F.P., Vermeulen, R.C.N., van Heck, J.G.A.M., Schoofs, A.J.G., van Campen, D.H.: Design of a Stroke Dependent Damper for the Front Axle Suspension of a Truck Using Multibody System Dynamics and Numerical Optimisation. *Vehicle System Dynamics* 38 (2002), pp. 85–101.

[12] Naude, A.F., Snyman, J.A.: Optimisation of Road Vehicle Passive Suspension Systems. Part 1. Optimisation Algorithm and Vehicle Model. *Applied Mathematical Modelling* 27 (2003), pp. 249–261.

[13] Naude, A.F., Snyman, J.A.: Optimisation of Road Vehicle Passive Suspension Systems. Part 2. Qualification and Case Study. *Applied Mathematical Modelling* 27 (2003), pp. 263–274.

[14] Naude, A.F.: Computer Aided Design Optimisation of Road Vehicle Suspension Systems, PhD Thesis. *University of Pretoria, South Africa* (2001).

[15] Giliomee, C.L., Els, P.S.: Semi-Active Hydro-pneumatic Spring and Damper System. *Journal of Terramechanics* 35 (1998), pp. 109–117.

[16] Gillespie, T.D.: Fundamentals of Vehicle Dynamics. *SAE* (1999).

[17] British Standards Institution: British Standard Guide to Measurement and Evaluation of Human Exposure to Whole-Body Mechanical Vibration and Repeated Shock. *BS6841* (1987).

[18] Reimpell, J., Stoll, H.: The Automotive Chassis: Engineering Principles. *Arnold* (1998).

[19] The International Organisation for Standardisation: Mechanical Vibration and Shock - Evaluation of Human Exposure to Whole Body Vibration, Part 1: General Requirements. *ISO 2631-1* (15 July 1997).

[20] Els, P.S.: The Applicability of Ride Comfort Standards to Off-Road Vehicles. 34^{th} *United Kingdom Group Meeting on Human Responses to Vibration Proceedings* (22–24 September 1999), pp. 281–292.

[21] The International Organisation for Standardisation: Road Vehicles - Test Procedure for a Severe Lane-Chane Manœuvre. *ISO 3888* (01 September 1975).

[22] Crolla, D.A., Chen, D.C., Whitehead, J.P., Alstead, C.J.: Vehicle Handling Assessment Using a Combined Subjective-Objective Approach. *SAE 980226*(1998).

[23] Dahlberg, E.: A Method Determining the Dynamic Rollover Threshold of Commercial Vehicles. *SAE 2000-01-3492*(2000).

[24] Els, P.S., Uys, P.E.: Investigation of the Applicability of the Dynamic-Q Optimisation Algorithm to Vehicle Suspension Design. *Mathematical and Computer Modeling* 37 (2003), pp. 1029–1046.

[25] Matlab Optimisation Toolbox Users Guide Version 2.2. *Mathworks* (2000).

[26] Han, S.P.: A Globally Convergent Method for Nonlinear Programming. *Journal of Optimization Theory and Applications* 22 (1977), pp. 297.

[27] Powell, M.J.D.: A Fast Algorithm for Nonlinearly Constrained Optimization Calculations. *Numerical Analysis, G.A.Watson ed., Lecture Notes in Mathematics, Springer Verlag* 630, (1978).

[28] Snyman, J.A.: A New and Dynamic Method for Unconstrained Minimisation. *Applied Mathematical Modelling* 6 (1982), pp. 449–462.

[29] Snyman, J.A.: The LFOPC Leap-Frog Algorithm for Constrained Optimisation. *Computers and Mathematics with Applications* 40 (2000), pp. 1085–1096.

[30] Snyman, J.A., Hay, A.M.: The Dynamic-Q Optimisation Method: An Alternative to SQP?. *Computers and Mathematics with Applications* 44 (2002), pp. 1589–1598.

[31] Vanderplaats, G.N.: Numerical Optimization Techniques for Engineering Design: With Applications. *McGraw-Hill* (1984).

[32] Eriksson, P., Friberg, O.: Ride Comfort Optimisation of a City Bus. *Structural and Multidisciplinary Optimisation* 20 (2000), pp. 67–75.

[33] Arora, J.S.: IDESIGN User's Manual, Version 3.5.2. *Technical Report ODL-89.7, College of Engineering, The University of Iowa, Iowa City* (1989).

[34] Eriksson, P., Andersson, D.: Handling and Ride Comfort Optimisation of an Inter-city Bus. *IAVSD'03 Conference* paper 63 (August 2003).

[35] Parkinson, A., Wilson, M.: Development of a Hybrid GRG-SQP Algorithm for Constrained Nonlinear Programming. *Journal of Mechanisms, Transmissions, and Automation in Design (now Journal of Mechanical Design), Transactions of ASME* 110 (September 1988), pp. 308.

[36] Gobbi, M., Mastinu, G., Doniselli, C., Guglielmetto, L., Pisino, E.: Optimal and Robust Design of a Road Vehicle Suspension System. *Vehicle System Dynamics Supplement* 33 (1999), pp. 3–22.

[37] Gobbi, M., Mastinu, G., Doniselli, C.: Optimising a Car Chassis. *Vehicle System Dynamics* 32 (1999), pp. 149–170.

[38] Gobbi, M., Mastinu, G.: Analytical Description and Optimisation of the Dynamic Behaviour of Passively Suspended Road Vehicles. *Journal of Sound and Vibration* 245 (2001), pp. 457–481.

[39] Gobbi, M., Levi, F., Mastinu, G.: Multi-objective Robust Design of the Suspension System of Road Vehicles. *IAVSD'03 Conference* paper 61 (August 2003).

[40] Mathworld Wolfram Research Website; Eric Weisstein's World of Mathematics, Spearmen Rank Correlation Coefficient. *http://mathworld.wolfram.com/SpearmanRankCorrelationCoefficient.htm* (12 November 2003).

[41] Lehmann, E.L., D'Abrera, H.J.M.: Nonparametrics: Statistical Methods Based on Ranks. *Englewood Cliffs, Prentice-Hall*(1998).

[42] Schuller, J., Haque, I., Eckel, M.: An Approach for Optimisation of Vehicle Handling Behaviour in Simulation. *Vehicle System Dynamics Supplement* 37 (2002), pp. 24–37.

[43] The International Organisation for Standardisation: Road vehicles - Vehicle Dynamics Test Methods - Part 1: General Conditions for Passenger Cars. *ISO 15037-1* (1998).

[44] Eberhard, P., Schiehlen, W., Bestle, D.: Some Advantages of Stochastic Methods in Multi-criteria Optimisation of Multibody Systems. *Archive of Applied Mechanics* 69 (1999), pp. 543–554.

[45] Datoussaid, S., Verlinden, O., Conti, C.: Application of Evolutionary Strategies to Optimal Design of Multibody Systems. *Multibody System Dynamics* 8 (2002), pp. 393–408.

[46] Baumal, A.E., McPhee, J., Calamai, P.H.: Application of Genetic Algorithms to the Optimisation of an Active Vehicle Suspension Design. *Computer Methods in Applied Mechanics and Engineering* 163 (1998), pp. 87–94.

[47] Getting Started Using ADAMS/View, Version 12. *Mechanical Dynamics* (2002).

[48] Stipinovich, J.: Modelling and Validation of Anti-roll Bars in Adams. *MGV732 Advanced Vehicle Engineering Project* University of Pretoria (2002).

[49] Genta, G.: Motor Vehicle Dynamics: Modelling and Simulation. *World Scientific* (1997).

[50] Sharp, R.: Private discussion. *IAVSD'03 Conference* (2003).

[51] Craig, K., Venter, P.J., de Kock, D.J., Snyman, J.A.: Optimisation of Structural Grid Spacing Parameters for Separated Flow Simulation Using Mathematical Optimisation. *Journal of Wind Engineering and Industrial Aerodynamics* 80 (1999), pp. 221–231.

[52] Venter, P.J.: Optimisation of Grid Spacing and Turbulence Modelling Parameters for Atmospheric Flows, MEng thesis. *University of Pretoria, South Africa* (1999).

[53] Craig, K., de Kock, D.J., Snyman, J.A.: Using CFD and Mathematical Optimisation to Investigate Air Pollution Due to Stacks. *Journal of Numerical Methods in Engineering* 44 (1999), pp. 551–565.

[54] Uys, P.E., Els, P.S., Thoresson, M.J.: Validation of Handling Criteria. *9th European ISTVS Conference Proceedings* September (2003).

[55] Theron, N.J., Els, P.S.: Modelling of a Semi-active Hydro-pneumatic Spring-Damper System. *9th European ISTVS Conference Proceedings* September (2003).

APPENDIX

A. EVALUATION OF THE HANDLING OBJECTIVE FUNCTION

A.1 The Concern

From the beginning of this research there was mounting concern as to what parameter must be used for the handling objective function on a smooth surface. Must it be a combination of variables or just one single variable. If so which ones should be considered? In the preliminary study by Els and Uys [24], the roll angle was minimized in order to achieve optimum handling.

A.2 Tests Performed

Due to this uncertainty it was decided to do some basic driving tests. The tests consisted of 3 vehicles and 4 drivers. The vehicles were a Ford Courier LDV, a VW CitiGolf 1 Chico, a VW Golf 4 GTi. These vehicles were chosen due to their availability and their handling characteristics ranging from almost nonexistent to excellent. The vehicles were instrumented to measure lateral acceleration front and rear, roll, pitch and yaw velocity, roll and pitch angle, vertical acceleration front and rear, longitudinal acceleration front and rear, as well as vehicle speed and steering wheel angle. Table A.1 summarizes the instrumentation fitted to the vehicles. The pack of drivers consisted of a student, a lady, and two men. The tests were performed on two tracks at Gerotek being the ride and handling track and the dynamic handling track. The ride and handling track simulates typical tarred mountain pass driving. The ride and handling track simulates typical high speed manœuvring. The track specifications are summarized in Table A.2.

Table A.1: Summarized vehicle measurements

Instrument	Position	Measurement
Accelerometer	Front Center	Lateral, Longitudinal, Vertical Accelerations
Accelerometer	Right Rear	Lateral, Longitudinal, Vertical Accelerations
Accelerometer	Left Rear	Lateral, Longitudinal, Vertical Accelerations
Angle sensor	Front Center	Roll, Pitch Angles
Gyro	Left Center	Roll, Yaw, Pitch Velocities
Displacement	Steering System	Steering Wheel Angle
Speed	Rear	Longitudinal Speed

A.3 Results From Study

The following trends relating to the handling can be observed in Figures A.1-A.4:

- Non-linear relation between vehicle speed and lateral acceleration
- Linear relation between roll angle and yaw velocity
- Linear relation between yaw velocity and lateral acceleration
- Linear relation between roll angle and lateral acceleration

These trends were the same for all drivers on both tracks in all the vehicles. The absolute values differed from driver to driver and vehicle to vehicle. The most important is the linear relation observed between roll angle, yaw velocity and lateral acceleration. This means for the purpose of optimisation of handling on a smooth surface either roll angle, yaw velocity or lateral acceleration may be used for the objective function. Roll angle was chosen as it is a visible improvement. Figure A.5 illustrates the standard Land Rover Defender while completing the double lane change, note the amount of body roll.

Table A.2: Test track specifications

Ride and Handling Track
Designed to evaluate ride and handling characteristics and driveline endurance of wheeled vehicles. Simulating typical tarred mountain passes.
Distance: 4.2 km
Turns: 13 left 15 right
Max gradient: 15 percent
Dynamic Handling Track
Designed to evaluate the high speed handling characteristics of light vehicles.
Distance: 1.68 km
Track surface: Asphalt
Coefficient of Friction: 0.7 average
Consisted of trapezium curve, spiral curve, kink/hairpin combination, high speed sweep

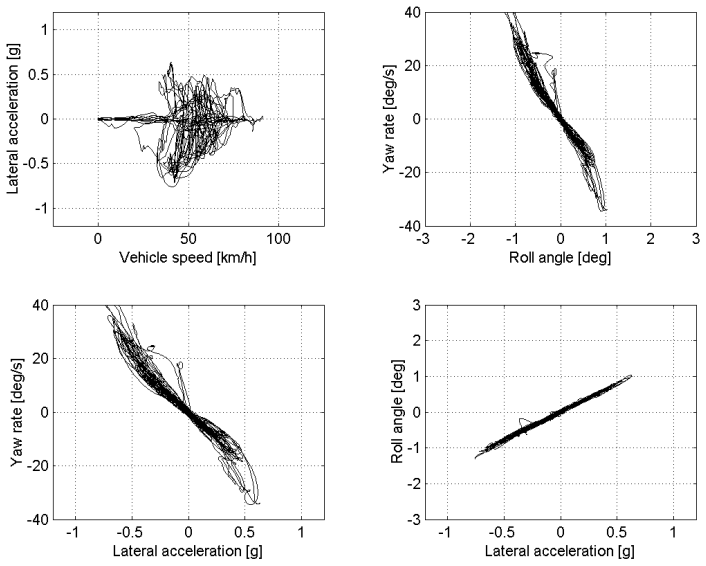

Figure A.1: Different drivers in Ford Courier on dynamic handling track

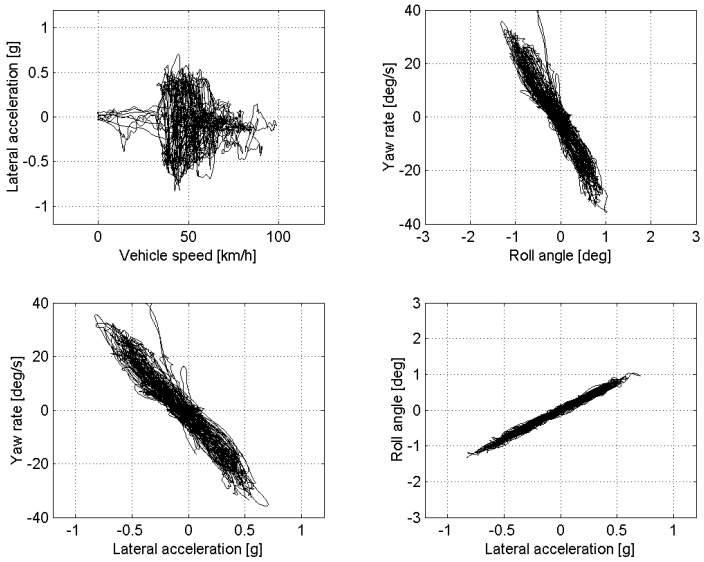

Figure A.2: Different drivers in Ford Courier on ride and handling track

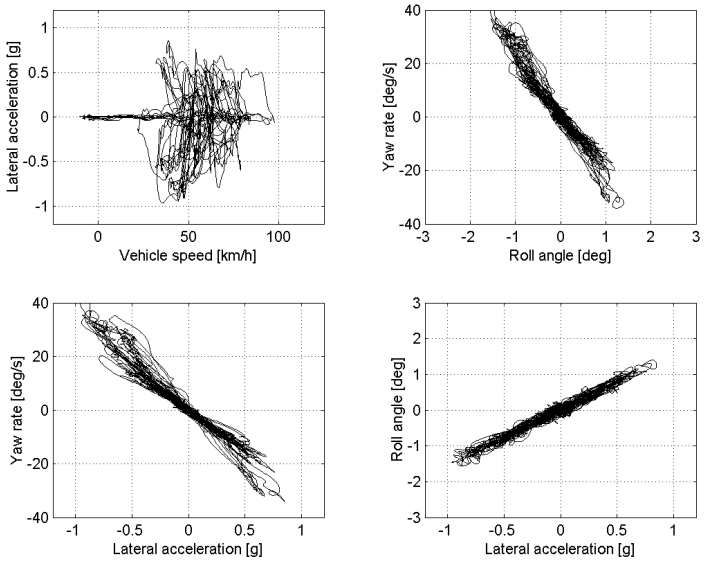

Figure A.3: Different drivers in VW Golf 4 GTi on dynamic handling track

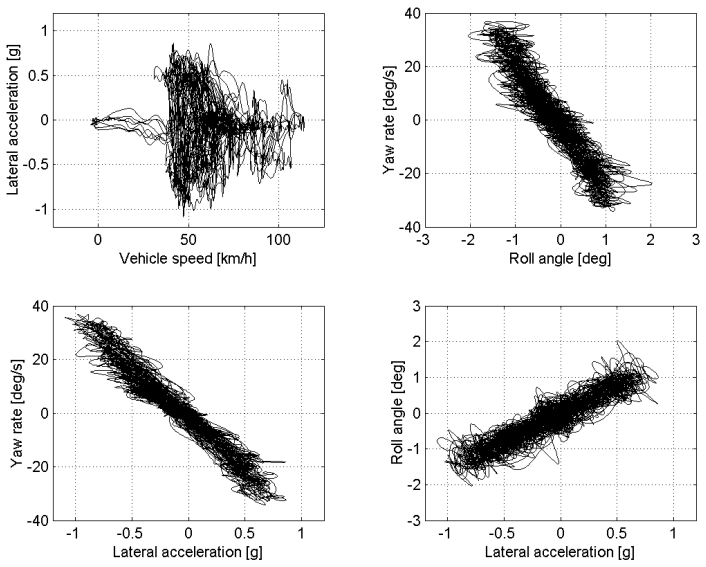

Figure A.4: Different drivers in VW Golf 4 GTi on ride and handling track

Figure A.5: Standard Land Rover Defender in double lane change manœuvre